Spatial and temporal variations in glacier aerodynamic surface roughness during the melting season, as estimated at August-one ice cap, Qilian mountains, China

Junfeng Liu et al.

Dear Editor,

We have carefully revised the manuscript according to the comments from referee #1 and #2. The most important comments are that 1) misunderstanding of surface roughness with aerodynamic surface roughness; 2) unclear of method part; 3) precision problem of manual and automatic photogrammetry; 4) ice surface is cryoconite or red snow algae? 5) Figures does not meet the high quality standards of TC.

We have given some carful explanations in our reply; please see the detailed point-by-point responses below. The corresponding changes have been made in the revised paper, track changes was used in order to be easily identified. Marked-up manuscript was given at the end of the replies. We hope the revised manuscript is suitable for the journal.

Best regards,

Junfeng Liu

Reply to comments from referee Joshua Chambers

General comments:

In this study, which is well within the remit of the journal, the authors present some interesting, hard-won (by the sounds of it) microtopographic and meteorological data from the August-one ice cap, China. They implement novel methods to collect some of their photogrammetric data automatically, in a location that is underrepresented in the glaciological literature.

Methods and data are presented and explained reasonably clearly, with some valuable insights given through comparison between microtopographic and meteorological measurements. While there is no independent validation of z0 values with other methods of obtaining z0 (wind profiles, eddy covariance), this is one of few studies that shows how the microtopographic methods used here can produce sensible values for melt volumes in the wider context of glacier monitoring. The temporal aspect of the work is a worthwhile inclusion, not just for the interesting nature of the data, but for the implications if such patterns were observed/studied elsewhere.

Overall it is well written and structured logically, and does not need much revision to make it publishable. Suggestions are fairly minor, although I would suggest that:

1) some terminology should be adjusted (see specific comments regarding 'surface roughness', 'direct measurement' etc), 2) methods need further justification, in that some additional studies should be read/cited (again, see specific comments) and 3) figures could be of higher quality generally (i.e. do not just use screenshots for com- pound figures).

Reply: In the revised version of the paper, we adjusted the terminology of 'surface roughness' as 'aerodynamic surface roughness'. In the methods part, we cite these latest studies. Figures in the revised version have higher quality.

Specific comments:

Abstract seeing as your work relates to z0 and not albedo, I would remove the mentions of albedo from the abstract to avoid confusion.

Reply: We delete accordingly.

Introduction

Line 32: here, and throughout the manuscript, make sure to add a space between citations listed in parentheses and separated by semi-colons.

Reply: Done

Line 41 – missed references to more recent studies using wind profiles:

Miles, E.S., Steiner, J.F. and Brun, F., (2017). Highly variable aerodynamic roughness length (z0) for a hummocky debris-covered glacier. Journal of Geophysical Research: Atmospheres, 122(16), pp.8447-8466.

Quincey, D., Smith, M., Rounce, D., Ross, A., King, O. and Watson, C., (2017). Evaluating morphological estimates of the aerodynamic roughness of debris covered glacier ice. Earth Surface Processes and Landforms, 42(15), pp.2541-2553.

Reply: Thanks for your suggestions, we cited related literatures as

Miles, E.S., Steiner, J.F. and Brun, F., (2017). Highly variable aerodynamic roughness length (z0) for a hummocky debris-covered glacier. Journal of Geophysical Research: Atmospheres, 122(16), pp.8447-8466. doi:10.1002/2017JD026510

Quincey, D., Smith, M., Rounce, D., Ross, A., King, O. and Watson, C., (2017). Evaluating morphological estimates of the aerodynamic roughness of debris covered glacier ice. Earth Surface Processes and Landforms, 42(15), 2541-2553. DOI:10.1002/esp.4198.

Line 42 – "direct measurement of z0 has been shown to be more accurate than previ- ous methods" – it is unclear what methods are referred to by this statement. Wind pro- file and microtopographic values are both estimates based on models. Please clarify or correct, and make sure it is clear throughout the rest of the paper that microtopographic z0 is an estimate, not a measurement.

Reply: Thanks for your suggestions. We delete the sentence in Line 42 and rewrite as "Glacier surface z_0 has been widely studied through methods such as eddy covariance (Munro, 1989;Smeets et al., 2000;Smeets and Van den Broeke, 2008; Fitzpatrick et al., 2019), or wind profile (Wendler and Streten, 1969; Greuell and Smeets, 2001; Denby and Snellen, 2002; Miles et al., 2017; Quincey et al., 2017). However, micro-topographic estimated z_0 shows some advantages, such as lower scatter, rather than profile measurements over slush and ice (Brock et al., 2006), and ease of application at different locations (Smith et al., 2016)."

The "direct measurement" changed to "microtopographic estimated z0". The rest of the paper also changed accordingly.

Line 44 – "Current research has increasingly used direct measurement." Terminology needs adjusting to reflect the previous comment.

Reply: Done.

Line 47 – as above.

Reply: Done.

Line 49 – 51: The first sentence could be backed-up by several examples including Irvine-Fynn et al (2014), Smith et al (2016), Quincey et al (2017), Miles et al (2017), and Fitzpatrick et al (2019). The second and third sentences are confusing; while Kääb and Vollmer (2000) utilised aerial photography for photogrammetry, this was not used for a purpose related to ice roughness. The next sentence "Digital photos were taken against a dark background plate" does not refer to a part of the cited study, but rather to Rees (1999), who published the method mentioned.

Reply: We added these references in the first sentence.

The following part has changed as 'Initially, the Micro-topographic method was developed as snow digital photos were taken against a dark background plate. The contrast between the surface photo and the plate could then be quantified as an estimation of surface roughness (Rees, 1998). This method is still widely applied to quantify glacier surface roughness (Rees and Arnold, 2006; Fassnacht et al., 2009a; Fassnacht et al., 2009b; Manninen et al., 2012).'

Data and methods – overall this is very clear, and the photogrammetry details are nice to

see.

Line 72: it would be interesting and useful background to include some information on the normal influence of the turbulent fluxes at this location.

Reply: we cited one published energy balance analysis results by Qing et al., (2018). The add part "Energy balance analysis indicated that net radiation contribute 86% and turbulent heat fluxes contribute about 14% to the energy budget in the melting season. A sustained period of positive turbulent latent flux exists on the August-one ice cap in August, causing faster melt rate in this period (Qing et al., 2018)."

Figure 1: Some scale would be useful in both panels. Is the figure a screenshot? Some artefacts have made their way into the top of the figure. Also some place names for context in panel (a) would help.

Reply: Done

Line 93-94: Figure 2b does not illustrate the frame very well, in fact it is quite unclear what the image shows.

Reply: we have revised accordingly.

In the revised manuscript, We split Figure 2 to Figure 2 and Figure3. Figure 2 showed the automatic photogrammetry. Figure 3 illustrate the automatic and manual photogrammetry control points and check points, the control frame, and the detrended DEM.

Line 99: in which direction did the camera move? Along the frame, or into it?

Reply ： The camera was 1.7m above ice surface and move along the control frame.

Line 117: what was the rationale for the plot size?

Reply：Plots should large enough to include obstacles to represent the glacier surface. The August-one glacier ice cap is generally smooth and uniform surface. We expect the 1.1*1.1m plot is large enough to represent the dominant roughness elements influencing z0. Additionally, the 1.1m*1.1m aluminum square is quite portable and easily apply at different locations of glacier.

Figure 2: do you have any other site photos? Panel (b) is not very useful as it is, and some detail is not shown by panel (3).

Reply: we have used photo and corresponding DEM data to represent the manual and automatic photogrammetry acquired micro-scale surface roughness.

Line 131: it might be useful to refer to the work of James & Robson (2014) and James et al (2017) for some critiques of using Agisoft Photoscan.

Reply: Done

In this part, we cite James & Robson (2014) and James et al (2017) for some critiques of using Agisoft Photoscan. We also include two debris-covered glacier z0 estimation paper based on Agisoft.

The new paragraph rewrite as "Structure-from-motion photogrammetry is revolutionizing the collection of detailed topographic data (Westoby et al., 2012; James et al., 2017). High resolution DEMs produced from photographs acquired with consumer cameras need careful handling (James and Robson, 2014). In this study, both manual and automatically derived photographs were imported into a software program, Agisoft Photoscan Professional 1.4.0. This software allowed us to estimate camera intrinsic parameters, camera positions, and scene geometry. Agisoft Photoscan Professional is a commercial package which implements all stages of photogrammetric processing (James et al., 2017). It has previously been used to generate three-

dimensional point clouds and digital elevation models of debris-covered glaciers (Miles et al., 2017; Quincey et al., 2017; Steiner et al., 2019), ice surfaces and braided meltwater rivers (Javernick et al., 2014; Smith et al., 2016). In our study, we found that after new snowfall, it was difficult to match feature points in the photo sets. Three days of automatic data could not be processed. We estimated z_0 data for the missing days based on data from snowfall days at the automatic site."

Line 149: repetition of reference.

Reply: Done

Line 156: Smith et al (2016) calculated h* from the mean vertical extent above a de-trended plane. Hopefully this important step has just been omitted from the text (in which case it should be added, as detrending is a vital part of the method), and not from your calculations.

Reply: For manual observation, the aluminum frame laid horizontally over the glacier surface. For automatic observation, the control field was also laid horizontally over the ice surface that lowered as the ice melted, and maintained a horizontally position between control field and ice surface. We have add the detrend method in line 565 as 'For manual photogrammetry, we put the aluminum frame horizontally over the ice surface, the plot is detrended by setting the control points at z axis of the same values. For automatic photogrammetry, the control field of wooden frame was also laid horizontally over the ice surface that lowered as the ice melted and maintained a horizontal position between the control field and ice surface. A DEM based approach enables the roughness frontal area *s* to be calculated directly for each cardinal wind direction (Smith et al., 2016). The combined roughness frontal area was calculated across the plot, the ground area occupied by micro-topographic obstacles is $1m^2$. We used a DEM-based average ($\bar{z}_{0\_DEM}$) of four cardinal wind directions to represent overall aerodynamic surface roughness. Based on the half-hour wind direction data at the August-one ice cap, the daily upward wind direction DEM-based z_{0_DEM} was also estimated at the automatic photogrammetry site. Considering that wind direction changed during the day, in this case we selected the prevailing wind direction to calculate frontal area *s*. The prevailing upwind direction DEM-based z_{0_DEM} was applied to calculate turbulent heat flux. Using the Munro (1989) method, $z_{0\_Profile}$ was calculated for every profile (n=1000) in both orthogonal directions for each plot at the automatic photogrammetry site. '

Line 162: please reference Munro (1989) for the profile-based simplification of the Lettau (1969) equation.

Reply: Done,

In the revised manuscript, we not only apply Munro(1989) method but also calculate the z0 based upward wind direction DEM based z0 to represent the aerodynamic surface roughness, and applied to calculate turbulent heat flux.

We have revised in the manuscript as 'Based on the work of Lettau (1969), Munro (1989) simplified the equation (1) by assuming that h* can equal twice the standard deviation of elevations in the de-trended profile, with the profile's mean elevation set to 0 meter. The aerodynamic roughness length for a given profile then becomes '

"

Line 174: Fitzpatrick et al (2019) also provide useful discussion of microtopographic methods. In addition, please clarify terminology – I would suggest reconsidering the use of the term 'surface roughness' as it can refer to one of a number of metrics (Smith, 2014), and could be more specific.

Reply: Thanks for your recommendation about Fitzpatrick et al (2019) study about microtopographic methods, which have provide EC comparsion with DEM based z0 in multi-season . This paper also give detailed introduction about z_0 estimation from DEM. We have referenced this paper in our study accordingly.

We add a sentence as line 152 as "Fitzpatrick et al. (2019) also developed two methods for the remote estimation of z_0 by utilizing lidar-derived DEM."

Consider the 'surface roughness' is not specific. We have revised the surface roughness as aerodynamic surface roughness in this paper.

Results

Section 3.1 Photogrammetry precision: while this is important to report, much of the text is summarised in the two tables and two figures. If you were looking to cut down on text, perhaps this section could be more concise.

Reply: we revised and provide uncertainty in the revised manuscript

Line 213: change geo-reference to geo-referencing. Also, I'm not sure which value is being referred to by saying that "errors were less than 1 millimeter", as most of the averages in the tables are >1 mm.

Reply: We agree, now the sentence is revised as "The average geo-referencing errors were fluctuate around 1 millimeter"

Line 216: define RMSE before the first use of the acronym (line 213), not after the second time.

Reply: We have changed accordingly.

Line 227: Note that the accuracy requirements given by Rees and Arnold (2006) were for 2D topographic transects, not 3D plots.

Reply: Thanks for remind, we delete this sentence accordingly.

Line 237: change 'covered' to 'covering'

Reply: Done

We have revised as' Data for ice surface roughness was collected from the automatic photogrammetry camera site from July 12 to September 15, a period covering the whole melting season.'

Line 237: "z0 was highly variable" – it's worth keeping some perspective here. While z0 varied, it did so by less than 3 mm.

Reply: We have revised accordingly.

Figure 5: There is a typo on the y-axis label which should read 'surface roughness'. Also please see my previous note on using the term 'surface roughness'.

Reply: We have changed as "Aerodynamic surface roughness"

Line 258: Should be 'both of which occurred in periods of transition'.

Reply: We have changed accordingly.

Line 261: This is an interesting finding. Can you provide more detail? Can you include the actual values for the manually collected data that show the same pattern? Addition- ally, in the methods it is mentioned that z0 is an average of all four directional values – were the individual values analysed for directional influence?

Reply: We did want analysis the four cardinal direction z_0 for manual data. But we did not strictly control the aluminum frame at certain direction during our field work at that time. We find at automatic site, at south to north direction z_0 seem larger than north to south direction z_0. We expect it is related with direct short wave radiation. We are not so sure. We need accumulate more field work to prove this.

In the revised manuscript of Figure 5, we have include DEM based four directions Z0 and prevailing wind direction z0. Munro profile method calculated z0 at two directions are also included.

Line 265: While z0 certainly changed over time, I do not think it is correct to say that it was related to the date. It was different when measured on different days, but this is because of factors other than what day of the month it is.

Reply: We totally agree. We have revised as 'Analysis indicated that $\bar{z}_{0\_DEM}$ proved to have an interesting relationship with altitude'

Line 268: is the 'terminal' the same as the terminus of the glacier? The latter expres- sion is more commonly used.

Reply: We have revised 'terminal' as 'terminus'

Line 269: Change to 'At higher altitudes'

Reply: Done

Line 275: Please be more specific than just saying "Manual investigation" – I take it here you are referring to photogrammetric data collected manually?

Reply: We totally agree, the sentence have revised as" Photogrammetric data collected manually revealed that ice surface roughness increased with altitude (Figure. 6c). From terminal to top, z_0 varied from 0.06 mm to 2.2 mm."

Lines 306-309: I am not sure that a separate introduction is required here. The final two sentences could be tacked onto the beginning of the next paragraph.

Reply: Agree. We have delete the first sentence and the final two sentences tacked onto the beginning of the next paragraph.

Line 335: changed "account" to "accounted".

Reply: Done

Line 360: the r2 value reported here is different to the one shown in Figure 9. This is also the case for line 370 and fig. 11a, and line 372/fig. 11b.

Reply: we showed r2 in In Figure 9, in line 360, we reported the correlation coefficient (r). In Figure 11a and Figure 11b, we also reported r2, and in line 370 we reported r instead of r2.

In the revised version, we reported r2 instead of r.

Discussion

Line 412: I do not think there needs to be a summary here – all of the information should be apparent from the main text.

Reply: We have revised the discussion part accordingly.

Line 414: Do not need to cite these again here.

Reply: Done

Line 416: I notice that the difference between ice z0 and snow z0 is very small. Can you comment on this in the text? Some find that the difference can be an order of mag- nitude. Were both surfaces at your site particularly smooth? Or could it be something to do with the size of the patch (thinking about the scale/resolution dependency of the microtopographic method – see Fitzpatrick et al. 2019).

Reply: we have revised this part and give some explanation why ice surface kept at certain domain during melting season, which is related with net shortwave radiation and turbulent heat flux. The former energy item seem increased z0. But turbulent heat flux seems smooth z0.

Lines 422-425: this paragraph needs rewording so that the first sentence does not seem disconnected from the rest.

Reply: we have revised accordingly

Lines 430-433: this is a significant finding; however, there is something about the word- ing in this sentence that I think should be addressed – as z0 is in this instance (using the bulk method) required to calculate the turbulent fluxes, arguing that the turbulent heat index (calculated with turbulent fluxes) is a determining factor seems circular. I think the statement could be made more clearly, perhaps referring to the association between the two rather than a causal relationship.

Reply: we have add the profile method and bulk method. Both method shown a similar relationship. A lagged correlation was also applied in the revised manuscript to indicate the

relationship between main energy items and z0.

Line 434: Make sure terminology is clear here – you refer to the August-one ice cap, and then call it a glacier. In my understanding, these are different.

Reply: we have revised accordingly. "the August-one glacier" changed to "the August-one ice cap" across whole manuscript.

Line 439: The second sentence can be deleted, it does not add anything to the findings or argument.

Reply: We have deleted the last sentence. The revised part has changed as" This study found an exponential relationship between z_0 and L_S. The delicate role of z_0 played in the ice surface balance is still not fully known. Further comparative studies are needed to investigate the z_0 variation through eddy covariance, profile method and DEM-based z_0 estimation."

Conclusion

I think comparison to other ice masses, and links to other studies/locations should be made in the discussion, with some thought given to whether you might find the same results where ice z0 and snow z0 have greater contrast. And, while it is important to acknowledge the site specificity of a study, further studies are always required and saying so in the conclusions is superfluous. Instead, the main messages from the paper (3 or 4 of them, as far as I can see) should be summarised here.

Reply: thanks for your suggestions. We have revised accordingly

Reply to comments from anonymous referee #2

The study by J Liu et al. demonstrates the first use of an automated photogrammetric apparatus to monitor surface roughness at a daily timescale for an ice cap in China. The authors supplement these observations from a single site with meteorological records from nearby, as well as manual photogrammetric measurements at a variety of locations across the ice cap during the course of the ablation season. The authors thus investigate spatial and temporal variations of surface roughness during the ablation season, as well as linkages to surface energy balance. From the automated roughness measurements they find that roughness is temporally variable and highly modified by precipitation, with both rain and snow precipitation leading to a reduction in roughness. From the manual measurements, they find that the seasonal firm/ice transition zone corresponds to the maximal surface roughness at any point, while ice or snow surfaces both exhibit lower surface roughness. The authors also suggest a link to the importance of turbulent fluxes in the whole energy balance.

The target of spatially-extensive surface roughness measurements is a novel development, and useful to understand roughness variations. While the general patterns of seasonal and spatial variability are very likely to be accurate and form a nice story, the authors seem to have some fundamental misunderstandings about surface roughness metrics and their meaning. In addition, the methods are not entirely clear, results are given to an unrealistic and misleading precision (also without any uncertainty assessment), and although the written English is generally correct, the writing style is particularly abrupt. Consequently, although the authors have painted a nice picture of the spatiotemporal evolution of surface roughness at August-one ice cap, the manuscript needs substantial revisions before it should be considered for publication in The Cryospehere.

Major points:

Fundamental misunderstanding of surface roughness. The authors seems to confuse Z_o and topographic surface roughness, which are not the same: while approaches have linked the two, the aerodynamic roughness length is not simply a topographic parameter, and efforts to assess Z_o based on topographic parameters need to be validated with micrometeorological measurements. Furthermore, the authors' effort to produce a grid-based estimate of surface roughness is only applicable for the case of isotropic roughness, which is not the case for ice surfaces.

Reply: Thanks for your comments. We have revised the manuscript based on your suggestions and comments. We have revised the topographic surface roughness as aerodynamic surface roughness (z_0) accordingly. For spatial and temporal z_0 variation, precisely capture wind direction data was not

available across the ice cap. In this case, we applied averaged four cardinal direction z_0 in the revised manuscript.

For the Anisotropy problem in here. We provide DEM based four cardinal direction z0 and Munro (1989) based profile method estimated z0 in Figure 5. Snow and ice surface photos were also provided to shown ice or snow surface features in Figure 5 and Figure 9. Glacier surface did showed some isotropic features. In order to avoid anisotropy in calculate turbulent heat flux, we estimated upwind z_0 by consider the prevailing wind direction data at top of ice cap. We have explained in the revised manuscript. The sensible and latent heat was calculated based on 4m half hour meteorological data and daily estimated prevailing wind direction z_{0_DEM}.

Lack of clarity with regards to several methods. The authors mention two specific efforts to estimate Z_o from topographic profiles: Lettau (1969) and Munro (1989). It is not clear which is actually used in this study, now how it was applied to the gridded height data. In addition, numerous details of the energy balance model used are missing, while the authors may have accidentally disregarded conduction of heat.

Reply: we have revised and clarify the detrend method and z_0 calculation. The Munro method was applied here in the revised manuscript. The subsurface heat flux was also calculated based on 8 level ice temperature observations deep down to 9.25m. The detrended method was presented in Line 566 of the revised manuscript. The upwind prevailing wind direction z_{0_DEM} was applied to calculate turbulent heat flux in Line 590 to 595. We also provided half-hour meteorological data in Figure 8 instead of daily scale meteorological data.

Unrealistic precision, no uncertainty of Z_o estimates or energy balance. The accuracy of Z_o is provided relative to control and check points on photogrammetric frames, and is reported to the tenth of a millimetre. However, it is unlikely that the actual measured positions of their control and check points are known to this accuracy. Furthermore, the surface height models produced by the structure-from-motion processing appear to be oversampled by a factor of 10x in each dimension, relative to the reported point densities. Finally, no assessment of uncertainty has been conducted for the Z_o estimates or the energy balance calculations.

Reply: The accuracy of check points and control points provided here are based on the Agisoft reports which provided precision information for each plot. In the revised manuscript, we have provided precision uncertainty about check points and control points in Figure 4. The oversampled by a factor of 10x in each dimension have revised from 0.1mm to 1mm.

The uncertainty of Z0 have conducted and provided in the revised manuscript. No evidence given of cryoconite, but of red algae. This may be a misunderstanding of some sort, but the authors refer multiple times

to the development of cryoconite and its effect on surface roughness, a phenomenon that would certainly explain some of the surface roughness dynamics that they observe. However, the first time cryoconite is mentioned is with regards to Figure 2, but Figure 2 does not provide any evidence (to my eye) of cryoconite – rather, red snow algae is clearly evident. This gives some concern of a basic misinterpretation of results.

Reply: we have provided evidence of photos in Figure 3 and Figure 5 to shown cryoconite. Two photos were also provided here to shown more detailed information about its size and ice surface cryoconite holes over August-one ice cap. Actually in the field work, we sampled surface cryoconite at 20cm *20cm plot, and dried it in the laboratory. Most of the substance was small mineral particles. The cryoconite appears red, it might related with it high concentration of Fe in it (Li et al., 2019).

For uncertainty of z0, we provide the uncertainty at Figure 3s, which is the mean of four cardinal direction z0 (Figure 3s a). The mean of Munro profile method calculated z0 was also provided (Figure 3s b). For the uncertainty of prevailing wind direction z0_DEM, we only acquired one data at every data. In this case we do not provide uncertainty in the revised manuscript.

Li Y, Kang S, Yang F, Chen J, Wang K, Paudyal R, Liu J, Qin X, Sillanpaa M, Cryoconite on a glacier on the north-eastern Tibetan plateau: light-absorbing impurities, albedo and enhanced melting. Journal of Glaciology, 65(252) 633-644.

Figure 1 Ice surface cryoconite and cryoconite holes.

Some grammar improvement needed, also some changes to the writing style are needed, as it is not currently suitable for TC.

Reply: Thanks for your suggestions, we have revised based on the detailed comments.

Detailed comments:

L1-2…during ‘the’ melting season

Reply: we agree. Now add 'the' as suggested.

L18. Zo was calculated from this data – you need to say how. Manual measurements of what type? Micrometeorology? Profiles of elevation difference?

Reply: We totally agree. This sentence has revised as: 'Z_0 was estimated based on microtopographic methods from automatic and manual photogrammetric data.'

L37-63. It is apparent from this section that the authors misunderstand several key concepts relating to Zo and turbulent heat transfer more generally; I suggest a careful read of Smith et al (2016) for a review of the differences. First, Z_o may be commonly called 'surface roughness' but its full title is the 'aerodynamic roughness length' (for momentum transfer/heat transfer). In any case, it emerges in the bulk aerodynamic approach as a constant of integration that results from the interaction of the boundary layer with the surface. It is a meteorological term (not a topographical term) that is influenced by both properties of the boundary layer and the surface. One can determine an effective surface roughness 'directly' from eddy covariance measurements (and less directly from wind towers), but it is highly variable in time primarily because the boundary layer is often highlyvariable. The variability of the boundary layer leads to a different fetch over which the layer is interacting with the surface topography. The microtopographic roughness (which you have calculated) is thus a very good indication of Z_o, but the relationship is not direct or linear, as the energy balance is controlled not just by surface topography at an individual location, but is variably influenced by its surroundings (e.g. Steiner et al, 2019). Thus, it is difficult to trust the values of Z_o produced by this study, as they are not validated by wind tower or eddy covariance observations (which actually resolve Z_o). However, microtopographic roughness metrics are a very strong proxy for Z_o (e.g. Nield et al, 2013), so I have much more confidence in the temporal and spatial variability presented by the authors. However, I think they need to very carefully reframe their introduction to conform with established theory.

Reply: Thanks for your suggestion and comments. Your comments have greatly help us to revise this manuscript. We have revised 'surface roughness' as 'aerodynamic surface roughness'. The 'direct' or 'indirect measurement' have revised as 'estimated'. Because the location are different between the automatic photogrammetry observation and the wind tower. In this case, we did not shown the calculated z0 based on wind tower data. Actually, we have eddy covariance observations at the ice cap top since 2016. In 2019, we have move the microtopographic observation to the ice cap top in order to carry out comparison with wind tower and eddy covariance.

L42. Please provide references indicating that microtopographic Z_o is more accurate than wind profile or EC measurements. I don't know how one can claim this, as those methods are the 'ground truth' of Z_o at a site.

Reply: We made a mistake here. The estimation of z0 based on microtopographic method showed some

advantages over EC measurements or profile methods rather than more precise.

We have revised this part as "However, micro-topographic estimated z_0 shows some advantages such as lower scatter than profile measurements over slush and ice (Brock et al., 2006), and easily application at different locations (Smith et al., 2016)""

L47. 'Direct measurement' is strange nomenclature; microtopographic approaches, including the Lettau (1969) approach, are anything but direct.

Reply: We fully agree and revised the "direct measurement" as "microtopographic estimated z0". The rest of the paper also changed accordingly.

L52. Rees and Arnold (2006) is also sensible to mention here.

Reply: We have add accordingly.

L55. Other examples of this approach are Rounce et al (2015), Quincey et al (2017), and Miles et al (2017).

Reply: Thanks for your recommendation, we have added accordingly. L56. The photogrammetric approaches need validation, as the relationship between topographic roughness and aerodynamic roughness length is also affected by local meteorology (Nield et al, 2013).

Reply: Thanks for your valuable comments.

We have revised this part as 'Such data facilitate the distributed parameterization of aerodynamic surface roughness over glacier surfaces (Smith et al., 2016; Miles et al., 2017; Fitzpatrick et al., 2019) Precision of microtopographic estimated z0 also became an major concern, and lots of comparative studies with aerodynamic method (eddy covariance or wind towers measurements) carried out over debris-covered or no-debris covered glaciers. Some of the studies showed the difference was within an order of magnitude (Fitzpatrick et al., 2019) or strongly correlated (Miles et al., 2017).'

L74/Figure1. Both panels need a scale. The political map of China is irrelevant to the current study; of more relevance are dominant weather patterns and elevation, including areas outside China's claimed border. Furthermore there is no need to depict the South China Sea, which results in a very poor use of space. What is the polygon within China? It is not identified in the figure or caption.

Please provide information about the image of August-one in panel (b) – date, satellite, etc. Red and green are poor choices of color for icons in panel (b), as many people cannot distinguish between these two colors.

Reply：We have edited as suggested.

L79. Please provide sensor specifications and measurement uncertainties for the AWS.

Reply: Done

We add Table 1 as :

Table 1 Measurement specifications for the AWS located at the top of the glacier (4820 m a.s.l.). The heights indicate the initial sensor distances to the glacier surface; the actual distances derived from the SR50A sensor.

Variable	Sensors	Stated accuracy	Initial Height (m)
Air temperature	Vaisala HMP 155A	± 0.2ºC	2, 4
Relative humidity	Vaisala HMP 155A	± 2%	2, 4
Wind speed	Young 05103	± 0.3 m/s	2, 4
Wind direction	Young 05103	± 0.3º	2, 4
Ice temperature	Apogee SI-11	± 0.2ºC	2
Shortwave radiations	Kipp&Zonen CNR-4	± 10% day total	2
Longwave radiation	Kipp&Zonen CNR-4	± 10% day total	2
Surface elevation changes	Campbell SR50A	± 0.01 m	2
Precipitation	OTT Pluvio^2	± 0.1 mm	1.7

L81. The sensor measures relative surface height; it does not measure mass balance. Also in L104

Reply: We agree. We have revised L81 sentence as' Surface relative height is measured by a Campbell Scientific ultrasonic depth gauge (UDG) close to the AWS'

For Line 104. We used a hunting-video camera to take pictures of ice-surface gauge stakes near automatic photogrammetry site. We expect it is mass balance of the site. The Figure 1 shows the hunting camera and stake close to top of the August-one ice cap, and rough surface and stake captured by hunting camera at the automatic photogrammetry site on September 9 of 2018. For clarity, we have

revised the sentence in line 104 as 'Surface elevation changes caused by accumulation and ablation was measured by digital infrared hunting-video camera, which took pictures of ice-surface gauge stakes located near the automatic photogrammetry site.'

Figure 2 Left side photo shows hunting-camera and mass balance stakes close to top of the August-one ice cap, right side photo showed hunting camera photographed rough ice surface on September 8 of 2018 and ice surface stake gauge at the automatic photogrammetry site.

L83. There was a windbreak fence installed on the glacier?

Reply: The wind break fence was installed for the OTT Pluvio^2 precipitation gauge. For clarity, we have revised as' An all-weather precipitation gauge adjacent to the AWS measures solid and liquid precipitation'.

L94. How were the positions of the control and check points measured? You report accuracies relative to these positions of less than 1 mm, but I am not convinced that you could locate the control point positions to a higher accuracy than this. Also, how was the frame structure anchored?

Reply: The report accuracies relative to these positions of less than 1 mm did have some problems. We have revised it and add uncertainty of precision.

For manual photogrammetry, a 1.1×1.1m portable square aluminum frame was applied as control field.

Geo-reference of the point cloud was enabled using control points established by four cross-shaped screws on the four corners of aluminum frame. Four cross-shaped screws on the middle of aluminum rimes used as check points. The location of these screws was measured precisely with millimeter brand tape. The frame structure just put on the ice surface without anchored.

Figure 3 Aluminum frame used as control field for Geo-referece at August-one ice cap. The hummocky is covered by cryoconites (grey part is sun dried cryoconite, brown part is wet cryoconite).

For automatic photogrammetry, a wooden frame, 1.5 m wide, and 2 m long, was put on the ice surface. This frame served as a geo-reference control field (Figure. 2b). The wooden rectangle frame was made by 4 water proofed 3 m rulers. The frame was put on the ice surface and chained together with two aluminum stakes ahead of the automatic photogrammetry camera. The wooden frame stands freely on the glacier and sinks with the melting surface.

All the control points and check point are located at feature points of the wooden frame, and these points also measured very carefully with millimeter brand tape.

L102. Did you choose the daily best-exposed sets of photos manually or automatically? For days with multiple very clear photo sets, was there strong agreement in derived Z_o or a consistent diurnal variation?

Reply: We choose the best-exposed sets of photos manually. Cloudy or frosty weather affected automatic photogrammetry exposures, and heavy snowfalls resulted in a texture-less surface. We choose photos to avoid these bad weathers.

Detailed analysis of diurnal variation was not carried out yet. Since z0 highly affected by weather conditions, Snowfall, rainfall also affected, and Refreezing at night could also affect the ice surface z0.

L112. Does the August-one ice cap have an accumulation area?

Reply: We have observed for the last 5 years. No accumulation area for the ice cap.

L120. How are the seven pairs of convergent photos arranged? Do you use all 14 photos to produce the DEM and orthoimage? Did you ever carry out the manual photogrammetry at the automatic site?

Reply: We revised this part as:' Seven to twelve of such photos were taken at each survey site and surrounded the target area from different directions.'

We did not carried out manual photogrammetry at the automatic site.

L124/Figure 4. Panels b and c are switched relative to the text, which led to some confusion about the numbers of check points and control points. I see no evidence of cryoconite in the image, but of red algae which is commonly found on melting snow.

Reply: We have revised Figure 2.

In the revised manuscript, we split Figure 2 into Figure 2 and Figure 3. Figure 2 showed the automatic photogrammetry device. Figure 3 showed the control field and detrend DEM data.

In Figure2c, the cryoconite in the image was not clear. We have provide more clear evidence in revised Figure3c. The photo of Figure3c showed cryoconite hummocky, in which top of the mound were dry cryoconites, underneath were wet cryoconites. The color of cryoconite over August-one ice cap is not red, it is brown color.

L135. The standard reference for this processing workflow as applied to glaciers is Westoby et al (2012). Also, this approach has already been applied to estimate surface roughness of glacier surfaces: Quincey et al (2017), Miles et al (2017), Steiner et al (2019).

Reply: Thanks for your suggestions, we have revised and cited these references.

We revised as' Structure-from-motion photogrammetry is revolutionizing the collection of detailed topographic data (Westoby et al., 2012; James et al., 2017). High resolution DEMs produced from photographs acquired with consumer cameras needs handled carefully (James and Robson, 2014). In this study, both manual and automatic photographs were imported into a software program, Agisoft Photoscan Professional 1.4.0. This software allowed us to estimate camera intrinsic parameters, camera positions, and scene geometry. Agisoft Photoscan Professional is a commercial package which implements all stages of photogrammetric processing (James et al., 2017). It has previously been used

to generate three-dimensional point clouds and digital elevation models of debris-covered glaciers (Miles et al., 2017; Quincey et al., 2017), ice surfaces and braided meltwater rivers (Javernick et al., 2014; Smith et al., 2016). After new snowfall, it was difficult to match feature points in the photo sets. Three days of automatic data could not be processed. We estimated z0 data for the missing days based on data from snowfall days at the automatic site.'

L141-146. This content belongs in the background. Note that Lettau (1969) was the first such effort (of which I am aware). It is also worth noting the extensive review of microtopographic metrics by Nield et al (2013).

Reply: We have revised this part. The title of '2.5 Roughness calculation' has revised as '2.5 Aerodynamic roughness estimation'

The content of this paragraph has revised and referenced Lettau (1969) and Nield et al. (2013).

L145. Munro (1989) is probably the appropriate first reference here, as is Brock et al (2006).

Reply: We revised and add these two references accordingly.

L161. The method described (based on the standard deviation of detrended elevation) is precisely the Munro (1989) method.

Reply: In the revised manuscript, we referenced the Munro (1989) method.

We have revised as' Based on the work of Lettau (1969), Munro (1989) simplified the equation (1) by assuming that h* can equal twice the standard deviation of elevations in the de-trended profile, with the profile's mean elevation set to 0 meter. The aerodynamic roughness length for a given profile then becomes'

L172-3. Averaging over cardinal directions is only meaningful for surfaces that are isotropic. However, the literature has repeatedly shown that melting ice is strongly anisotropic, as the direction of wind strongly dictates the pattern of melt, and feeds back via roughness. So this 'averaging all cardinal profiles' is entirely unsuited to your study site, unless you can demonstrate that the ice surface is indeed isotropic in terms of roughness, which would be highly surprising.

Reply: We agree.

We have revised it as ' For manual photogrammetry, we put the aluminum frame horizontally over the ice surface, the plot is detrended by setting the control points at z axis of the same values. For automatic photogrammetry, the control field of wooden frame was also laid horizontally over the ice surface that lowered as the ice melted and maintained a horizontal position between the control field and ice surface. A DEM based approach enables the roughness frontal area s to be calculated directly for each cardinal wind direction (Smith et al., 2016). The combined roughness frontal area was calculated across the plot,

the ground area occupied by micro-topographic obstacles is 1m2. We used a DEM-based average ($\bar{z}_{0\_DEM}$) of four cardinal wind directions to represent overall aerodynamic surface roughness. Based on the half-hour wind direction data at the August-one ice cap, the daily upward wind direction DEM-based z0_DEM was also estimated at the automatic photogrammetry site. Considering that wind direction changed during the day, in this case we selected the prevailing wind direction to calculate frontal area s. The prevailing upwind direction DEM-based z0_DEM was applied to calculate turbulent heat flux. Using the Munro (1989) method, z0_Profile was calculated for every profile (n=1000) in both orthogonal directions for each plot at the automatic photogrammetry site.'

L174. Some things are not entirely clear to me about your method. First, do you use all profiles in each cardinal direction? Second, it is not clear if you have implemented the exact Lettau approach or the Munro approximation in your 'all profiles' approach. Third, such an implementation (all profiles averaged, for either Lettau or Munro) has already been implemented and tested for a glacier surface. Please see Miles et al, (2017).

Reply: We have used Lettau method for DEM based method, Munro method for profile method. The results was presented in Figure 5a. Average of four cardinal direction ($\bar{z}_{0\_DEM}$) and average of profile method (z0_Profile), the prevailing wind direction z0_DEM was all presented in Figure 5. z0_DEM was applied to calculate turbulent heat flux.

In the revised manuscript, we give detailed description in line 185 to 195, and line 210-215.

L179-181. The surface energy balance presented is not quite accurate for a 'melting' glacier, but for a 'temperate' glacier. Do you have any evidence that the August-one ice cap is temperate? If not, there also needs to be a term for heat conduction.

Reply: we have revised and add subsurface heat flux (QG) based on the observations at the ice cap. We have a subsurface temperature observation at five different depth. The maximum depth was 9.25m (beginning in 2015).

We have revised as 'The subsurface heat flux QG is estimated from the from the temperature-depth profile and is given by $Q_G = -k_T \frac{\partial t'}{\partial z'}$ where kT is the thermal conductivity, 0.4Wm-1K-1 for old snow and 2.2W m-1K-1 for pure ice (Oke, 1987).'

The result of Q_G was presented after rainfall energy in the revised manuscript as' Compared to other energy components, QG was very small, with a daily mean of -0.65 W m^{-2} and a maximum and minimum of -0.4 and -2.1 W m^{-2}, respectively.'

L191. My impression is that you use your calculated Z_o value for the bulk aerodynamic approach. How do

you integrate your 3-hourly (half-day) Z_o values with your model? At what timescale is the model run? What uncertainty does the input meteorology have, and what uncertainty does this produce for your results?

Reply: The turbulent heat flux was calculated based on half-hour meteorological data at 4m level and daily scale z_{0_DEM}. We assumed the z0 was same in each day. In the revised manuscript, we have revised it

We revised as 'In a horizontally homogeneous and steady surface state, the surface heat fluxes Q_E and Q_H can be calculated using either the bulk aerodynamic approach or profile method, based on the Monin-Obukhov similarity theory (e.g., ; Arck and Scherer, 2002; Garratt, 1992; Oke, 1987). In this study, half-hour observations at 4 m level and daily upward wind direction DEM-based z_0 were used to calculate Q_E and Q_H based on the bulk method.'

L204. Is an environmental lapse rate entirely appropriate for this site? Do you have lapse rate measurements?

Reply: We do not have lapse rate measurement here at the ice cap. We have applied temperature lapse rate of 5.6 ^{o}C Km^{-1} **observation results not far from here by Chen et al. (2014).**

We have revised as 'In order to calculate P_r, we used the air temperatures recorded at the AWS. There is an elevation difference between the study site (4700 m) and the AWS (4790m); recorded air temperatures were corrected to account for the elevation difference, a lapse rate of -5.6 ^{o}C Km^{-1} was applied based on observation nearby (Chen et al., 2014)'

L205. How confident are you that the AWS measurements are broadly representative of the entire ice cap? Do you have evidence to back up this claim?

Reply: the ice cap is flat and open terrain as shown in Figure1. The AWS is only 1500m away from the automatic photogrammetry site and 90m difference in altitude. This topographic feature favors the representative of the AWS over the ice cap.

We have revised this as' The ice cap is flat and open terrain so in this case wind speed and relative humidity at the study sites were assumed to be close to those observed at the AWS.'

L210-211. I am not sure how you get seventeen (17), as you have 4 control points and 3 check points. Similarly, I do not understand what the 31 manual photography pairs are – please explain.

Reply: we have revised as' We used seventeen plots to analyze the horizontal and vertical accuracy of our automatic photogrammetry, and thirty-one plots for our manual photogrammetry'

L210-219. This entire section is an amalgamation of bullet points; please rewrite to conform to style for The Cryosphere.

Reply: We have revised it.

L212 and L216. The reported point densities do not justify a resolution of 0.1mm, but of 1mm. These DEMs are 100x oversampled.

Reply: Agree, We have revised it accordingly.

L213. The average georeferenced error is greater than 1mm for half of the control points, and nearly all check points. However, I am also not certain how precisely you could have measured the location of the control and check points. Please provide details and uncertainty.

Reply: We have provide details at L94 for measurement of the control and check points. We aslo provide uncertainty for check points and control points in Figure 4.

L225. Yes, but part of this is also the difference of your survey design. For the automatic measurements, the camera is moving linearly, and the density of tie-points is much higher in the foreground compared to the background. For the manual method, although the survey design is not clear, more photos were taken and I presume that they surrounded the target area. This type of survey would be expected to provide a much more robust elevation model.

Reply: We agree. We have revised the manual survey was different from automatic photogrammetry. The manual survey surrounding the target, and automatic measurements moving linearly.

We have add this difference here and revised as' Note that the control and check point errors were larger for the automatic measurements than for the manual ones (See Figures 4). We believe that this is the case because, rather than using static f-stop and exposure times (as in automatic photogrammetry) researchers engaged in manual photogrammetry could adjust exposure time based on ice surface conditions. This allowed production of better quality photos even on cloudy or foggy days. The difference of survey design also caused more precise results for manual than automatic photogrammetry. For the automatic measurements, the camera was moving linearly, and the density of tie-points was much higher in the foreground compared to the background. For the manual method, photos were taken by surrounding the target area. This type of surface provided a much more robust elevation model and points density.'

L228. Rees and Arnold (2006) did indeed suggest millimetre vertical accuracy. The also suggest a fetch length of 3-6 meters as relevant for the majority of energy balance situations, which is considerably larger than your domain.

Reply: we have revised it. Rees and Arnold (2006) suggested millimeter vertical accuracy only for 1D

profile, not for 2D DEM data. The suggest a fetch length depend on the topography. In this study, a 1m square are more portable for manual photogrammetry. A lager plot scale need put camera 5-to 10 m or much higher locations to catch larger scale ice surface z_0. In this study we do not include larger plot scale comparative studies.

L230/Figure3. It is not clear what this chart shows – the y axis is labelled 'Differences', but is this RMSE, MAD, or…? Please clarify.

Reply: We have revised it as 'Standard derivation'.

L231-4/Figure 4. Same problem and Figure 3. Should be merged with Figure 3 as a second panel.

Reply: we have merged with Figure3, and revised as 'standard deviation'.

L238. No description of profile analysis is included in the manuscript, only of a DEM analysis. Please provide more detail.

Reply: We have provided more detail about profile results.

L239. Do you have an estimate of the uncertainty of these Z_o values?

Reply: For the average of four cardinal direction $\bar{z}_{0\_DEM}$ and Munro profile method calculated average of z0_Profile, We provide uncertainty in Figure 3s. For prevailing wind direction Z0_DEM. We do not have uncertainty because we have one data every day.

L242-254. Listing a narrative as bullet points in the results is not particularly aesthetic, and this section should be rewritten as a paragraph. More importantly, this section mixes results and interpretations. Please present the observations, then interpret them.

Reply: We have revised it as: 'At the start of the observation period of July 12, snow covered the study site. As the snow melted, the ice cap surface z0 increased. During this periods, z0 dropped to around 0.1mm due to intermittent snowfall. On July 21, cryoconite appeared on patches of snow-crust, which led to patchy melt. From July 21 to 24, overall z0 increased from 0.1mm to 1.6mm. By July 29, snow had disappeared from the study site, and z0 fluctuated but trended lower. From July 29 to August 5 bare ice covered whole field of view, and ice surface z0 ranged from 0.18 to 0.56mm. From August 6 to September 3 there was intermittent snowfall followed by melting, z0 ranged from 0.1 to 1.0mm. From September 4 to September 14 z0 showed an overall increase, reaching a maximum of 2.5 mm on September 8. There was intermittent snowfall during this period, which temporarily reduced z0. Z0 then increased due to patchy micro-scale melting. After September 14, snow covered the whole surface

of the ice cap. There was no melting and little fluctuation in z0.'

L254/Figure 5. Z_o values are more commonly presented on a logarithmic scale, as even a factor of 2 makes little difference in the turbulent fluxes, whereas a factor of 10 can be a considerable difference regardless of value. This is, in part, due to the bulk aerodynamic approach. Also, it would be very nice to include a set of panels depicting the surface at different parts of this record (high and low values, for example).

Reply: Thanks for your suggestions, we have revised accordingly.

L258. One order of magnitude is not a particularly large variation of Z_o.

Reply: We have revised as' It should be clear that z_0 varied from 0.05 to 2.74 during melting season'

L260. I have not yet seen evidence of cryoconite holes; the image in Figure 2 is unconvincing. Also applies to L280

Reply: We have add surface photos from July 12 to September 13 to show ice surface features at different periods in revised manuscript of Figure 5.

L263,276,277. I see no need to include p-values here.

Reply: we have revised it.

L274. Was there no accumulation in this year?

Reply: In August, at top of the ice cap, the mass balance is

already negative.

L283/Figure 6. Is there a reason that the lines are shown with different styles? For comparison, it would be good for all 4 panels to have the same y-axis limits.

Reply: we have revised it.

L288-302. Somewhere in this section there should be a reference to Figure 7.

Reply: we have revised and referenced Figure7

L310,324,353,339,345. The use of sub-headings here just breaks up the text.

Reply: We have deleted these sub-headings.

L320/Figure 7. In panel (a), please use a logarithmic scale for Z_o. Is panel (c) showing net solar radiation, or downwelling – not specified. The y-axis upper limit in panel (d) should be 100%. In general, all time-series look smoothed. Please provide details of exactly what is shown. In the caption, please be sure to provide the year.

Reply: we revised it accordingly.

L330/Figure 8. What is the uncertainty of each of these values quantities?

Reply: The Figure 8 displayed daily main energy items in which net radiation is calculated based on half hour observation of net shortwave radiation and net shortwave radiation. Latent and sensible heat is calculated based on half hour meteorological and daily windward direction DEM- estimated z_{0_DEM} (we assumed z0 is not changed during the day). The uncertainty is not included for simplicity. We have provide half-hour scale latent heat documents.

L335. If latent heat and sensible heat account for so little of the energy balance, how much impact does a variation of Z_o from 0.25 mm to 2.5 mm have on the total energy balance?

Reply: In this study, we calculated latent heat and sensible heat based on the bulk method. We do not include sensitive test of z0 variation on total energy balance. Actually we applied $z_{0\_Prifile}$, z_{0_DEM} and $\bar{z}_{0\_DEM}$ to the bulk method. Highly constant results was acquired between three different z0 (Figure 4s).

L343. The 'visible smoothing' is not clear to me from Figure 7. Please explain where you see this.

Reply: we have revised it and added two ice surface photos before rainfall and after rainfall event in Figure 9 to indicate the smoothing process.

L349-350. As turbulent fluxes matter very little for your energy balance, the match is not due to the calculated Z_o.

Reply: we agree. We have revised it accordingly.

L358-380/Fig10 and 11. I do not think this analysis is very well grounded in theory. First of all, as the turbulent fluxes depend on Z_o, you are comparing a quantity to a modified version of itself in Figure 10d and Figure 11. In fact, this exactly corresponds to the shape of the fit in bulk aerodynamic theory (which you have used to relate Z_o to the turbulent fluxes). So on one hand, none of this section is unexpected, but nor does it provide any novel insight. On the other hand, if you intend to examine the potential feedbacks between energy balance and surface roughness, that would be very interesting, but would require the use of a lagged correlation (in which case your variables would be independent).

Reply: Thanks for your excellent question and suggestions. We totally agree with you since Figure 11 and 12(revised manuscript) comparing DEM_ based z_0 with turbulent fluxes which were calculated based on it. In this case we have compared DEM-based z_{0_DEM}, $z_{0\_Profile}$, and $\bar{z}_{0\_DEM}$ with bulk method calculated turbulent fluxes to avoid the problem you mentioned. We also compared $z_{0\_Profile}$, and $\bar{z}_{0\_DEM}$ and main energy items, which all have similar results (Figure 1s and Figure 2s).

We have revised in method part as' Figure 11 shows the relationship between daily upward wind direction DEM-based z0_DEM and the main energy flows. Scatter diagrams showed a positive relationship between z0 and net shortwave radiation (Figure 11a, r=0.1) and a significant negative relationship between z0 and net longwave radiation (Figure 11b, r=-0.35), Graphing z0 vs. bulk method estimated latent heat showed a significant negative exponential relationship (Figure 11d, r= -0.35). The scatter diagram showed no significant relationship between z0_DEM and the bulk method estimated sensible heat (Figure 11c). The average of the Munro profile based z0_profile and DEM based $\bar{z}_{0\_DEM}$ and the main energy items are also analyzed respectively. Scatter diagrams showed significant negative relationship between z0_profile and net longwave radiation (Figure1s b, r=-0.5). Graphing z0_profile vs. the bulk method estimated sensible heat showed a significant negative exponential relationship (Figure 1s d, r=-0.69). These scatter diagrams showed no significant relationship between z0_Profile and the bulk method estimated sensible heat (Figure 11c, 11e). $\bar{z}_{0\_DEM}$ vs. the bulk method estimated latent heat showed a significant negative exponential relationship (Figure 2s d, r= -0.44). The scatter diagrams between $\bar{z}_{0\_DEM}$ and net shortwave radiation, the bulk method estimated sensible heat showed no significant relationship. '

L389. Again, Westoby et al (2012) is probably an even more appropriate reference here.

Reply: Thanks for your suggestion, we have revised and referenced Westoby et al (2012)

L391. I disagree with this because your survey setup is entirely different for the manual and automatic methods. See my comment with regards to L225.

Reply: We agree

We have revised it as 'We used both automatic and manual photogrammetric methods to sample spatial and temporal z_0 variation at the August-one ice cap. Adjust exposure time based on ice surface conditions and survey design of surrounding the target made the manual photogrammetry more precise than automatic photogrammetry (Tables 1 and 2). However, precision is not always the major concern. The glacier surface was a harsh, even punishing environment for the researchers doing manual photogrammetry. In addition, manual photogrammetry took much longer. Automatic methods reduced

hours of field work, spared researchers, and produced nearly continuous data. Cloudy or frosty weather affected automatic photogrammetry exposures, and heavy snowfalls resulted in a texture-less surface. Nevertheless, it is likely that photogrammetry techniques will continue to improve and that these drawbacks may be mitigated.'

L400. I believe you are referring to the glacier terminus. Please replace 'terminal' with 'terminus' throughout the manuscript.

Reply: We have revised it.

L403. This is the very interesting result of your study: following the zone of maximum roughness as it migrates upglacier. But a key question is how important are turbulent fluxes in this zone? Perhaps they are relatively unimportant everywhere else, but in this transition zone you have maximum Z_o and the zone also migrates across much of the glacier, highlighting the importance of transient surface characteristics.

Reply: Thanks for your comments. We have revised it based on your suggestions.

L429. Please be careful and consistent with the terminology that you use. In this study you have examined topographic roughness and the aerodynamic roughness length (which are not quite the same thing, see Smith et al, 2016).

Reply: we have revised topographic roughness as aerodynamic surface roughness.

L431. I do not think this is a meaningful result, see my comment on L358-380. This also applies to L439.

Reply: We have revised accordingly

L434. What do you mean by 'heavy-loading glacier'? I have not heard the term before.

Reply: we have revised it as' The August-one ice cap dust concentrations are high in melting season.'

L437. The link between cryoconite holes and surface roughness is indeed important, and you should make this link explicit earlier. However, your manuscript has not presented any clear evidence of the cryoconite development process occurring at your site.

Reply: We have provided ice surface photos to indicate this processes in Figure5.

L440. I do not understand what you are referring to here, with regards to quantitative vs qualitative research. Please explain more clearly what you are implying.

Reply: We have revised it

L456. What type of studies? Please make some concrete suggestions; at present this discussion and conclusion makes very little contribution to the field.

Reply: We have revised it accordingly.

605 L470 and L472. Duplicate reference.

Reply: We have revised it accordingly.

Spatial and temporal variations in glacier aerodynamic surface roughness during the melting season, as ~~observed~~ estimated at August-one ~~glacier~~ice cap, Qilian mountains, China

Junfeng Liu[1]*, Rensheng Chen[1], Chuntan Han[1]

[1] Qilian Alpine Ecology and Hydrology Research Station, Key Laboratory of Ecohydrology of Inland River Basin, Northwest Institute of Eco-Environment and Resources, Chinese Academy of Sciences, Lanzhou, China.

Correspondence to: Rensheng Chen (crs2008@lzb.ac.cn), Junfeng Liu (jfliu121@163.com)

Abstract: The aerodynamic roughness of glacier surfaces is an important factor governing ~~surface albedo and~~ turbulent heat transfer. Previous studies ~~have not directly observed~~rarely estimated spatial and temporal variation in aerodynamic surface roughness (z_0) over a whole glacier and whole melting season. Such observations can do much to help us understand variation in z_0 and thus variations in ~~albedo and~~ turbulent heat transfer. This study, at the August-one ice cap in the Qilian mountains, collected three-dimensional ice surface data at plot-scale, using both automatic and manual close-range digital photogrammetry. Data was collected from sampling sites spanning the whole ~~glacier~~ ice cap for the whole of the melting season. The automatic site collected daily photogrammetric measurements from July to September of 2018 for a plot near the center of the ice cap~~;~~. D~~d~~uring this time, snow cover gave place to ice and then returned to snow. z_0 was ~~calculated~~ estimated based on microtopographic methods from automatic and manual photogrammetric data~~from this data~~. Manual measurements were taken at sites dotted from terminals to top; they showed that z_0 was larger at the snow and ice transition zone than in areas fully snow or ice covered. This zone moved up the ice cap during the melting season. It is clear that persistent snowfall and rainfall both reduce z_0. Using data from a meteorological station near the automatic photogrammetry site, we were able to calculate surface energy balances over the course of the melting season. We found that high or rising turbulent heat as a component of surface energy balance tended to produce a smooth ice surface and a smaller z_0; low or decreasing turbulent heat tended to produce a rougher surface and larger z_0.

Keywords: aerodynamic surface roughness, digital photogrammetry, melting season, transition zone, surface energy balance, August-one ice cap

1. Introduction

The roughness of ice surfaces is an important control on air-ice heat transfer, on the ice surface albedo, and thus on the surface energy balance (Greuell and Smeets, 2001; Hock and Holmgren, 2005; Irvine-Fynn et al., 2014; Steiner et al., 2018). The snow and ice surface roughness at centimeter and millimeter scales is also an important parameter in studies of wind transport, snowdrifts, snowfall, snow grain size, and ice surface melt (Bruce and Smeets, 2000; Brock et al., 2006; McClung and Schaerer, 2006; Fassnacht et al., 2009a; Fassnacht et al., 2009b). Radar sensor signals, such as SAR (Oveisgharan and Zebker, 2007), altimeters and scatter meters, are also affected by ice and snow surface roughness (Lacroix et al., 2007; Lacroix et al., 2008). One of the most important of these influences is the aerodynamic roughness of z_0, which is related to ice surface topographic roughness in a complex way (Andreas, 2002; Lehning et al., 2002; Smith et al., 2016). Determination of z_0 based on topographic roughness is therefore of great interest for energy-balance studies (Greuell and Smeets, 2001).

Glacier surface z_0 has been widely ~~but indirectly~~ studied through such methods as eddy covariance (Munro, 1989; Smeets et al., 2000; Smeets and Van den Broeke, 2008; Fitzpatrick et al., 2019), or wind profile (Wendler and Streten, 1969; Greuell and Smeets, 2001; Denby and Snellen, 2002; Miles et al., 2017; Quincey et al., 2017). However, ~~direct measurement~~micro-topographic estimated ~~of~~ z_0 ~~has been shown to be more accurate than previous methods.~~shows some advantages, such as ~~Micro-topographic measured z_0 shows~~ lower scatter, rather than profile measurements over slush and ice (Brock et al., 2006), and ease of application at different locations (Smith et al., 2016). ~~.~~ ~~Current~~ research has increasingly used micro-topographic method to estimate z_0. ~~direct measurement.~~ It has also become clear that it is important to ~~measure~~ estimate z_0 over the entire course of the melting season and at many points on the glacier surface, as z_0 is prone to large spatial and temporal variation (Brock et al., 2006;Smeets and Van den Broeke, 2008). This variation is due to variations in weather and snowfall (Albert and Hawley, 2002). The ~~direct measurement of~~micro-topographic estimated z_0 allows repeated measurement at many points on the glacier surface, which is not possible with wind profile or eddy covariance methods.

Photogrammetry has been increasingly popular as a method to measure the aerodynamic surface roughness of snow and ice (Irvine-Fynn et al., 2014; Smith et al., 2016; Miles et al., 2017; Quincey et al., 2017; Fitzpatrick et al., 2019).~~surfaces roughness~~. Initially, the Micro-topographic method was developed as snow digital photos were taken against a dark background plate.~~The first use of the technique involved aircraft-mounted cameras on craft flying over snow and ice (Kääb and Vollmer, 2000). Digital photos were taken against a dark background plate.~~ The contrast between the surface photo and the plate could then be quantified as a measure of glacier roughness (Rees, 1998). This methods still widely applied to quantify glacier surface roughness (Rees and Arnold, 2006; Fassnacht et al., 2009a;Fassnacht et al., 2009b;Manninen et al., 2012). A more recent method, as described by Irvine-Fynn et al. (2014), uses modern consumer-grade digital cameras to do close-range photogrammetry at plot scale (small plots of only a few square meters). Appropriate image settings and acquisition geometry allow the collection of high-resolution data (Irvine-Fynn et al., 2014; Rounce et al., 2015; Smith et al., 2016; Miles et al., 2017; Quincey et al., 2017)~~(Irvine-Fynn et al., 2014;Smith et al., 2016)~~. ~~Such data allows researchers to investigate roughness with ever-greater precision.~~ Such data facilitates the distributed parameterization of aerodynamic surface roughness over glacier surfaces (Smith et al., 2016; Miles et al., 2017; Fitzpatrick et al., 2019). Precision of microtopographic estimated z_0 also became a major concern, and many comparative studies with the aerodynamic method (eddy covariance or wind towers

measurements) were carried out over debris-covered or non-debris covered glaciers. The difference was within an order of magnitude for some studies (Fitzpatrick et al., 2019) or strongly correlated (Miles et al., 2017).

Previous researchers have performed some long-term, systematic~~, direct~~ studies of glacier surfaces (Smeets et al., 1999; Brock et al., 2006; Smeets and Van den Broeke, 2008; Smith et al., 2016). The current study applied such methods to the study of snow and ice aerodynamic surface roughness during melting season at the August-one ice cap. We used both automatic digital photogrammetry and manual photogrammetry. Automatic methods allowed us to monitor daily variations in aerodynamic surface roughness; manual methods allowed us to characterize aerodynamic surface roughness~~surface~~ variation along the main glacial flow line. We also recorded meteorological observations, so as to study the impact of weather conditions (e.g. snowfall or rainfall) on aerodynamic surface roughness. This data allowed a further effort to characterize variation of plot-scale z_0 from an energy balance perspective.

2. Data and methods

2.1 Study area and meteorological data

The August-one glacier ice cap is located in the middle of Qilian Mountains on the northeastern edge of the Tibetan Plateau (Figure 1a, 1b). The glacier is a flat-topped ice cap that is approximately 2.3 km long and 2.4 km^2 in area. It ranges in elevation from 4550 to 4820m a.s.l. (Guo et al., 2015). This study was conducted during the melting season of 2018, a season characterized by high precipitation. Energy balance analysis indicated that net radiation contribute 86% and turbulent heat fluxes contribute about 14% to the energy budget in the melting season. A sustained period of positive turbulent latent flux exists on the August-one ice cap in August, causing faster melt rate in this period (Qing et al., 2018).

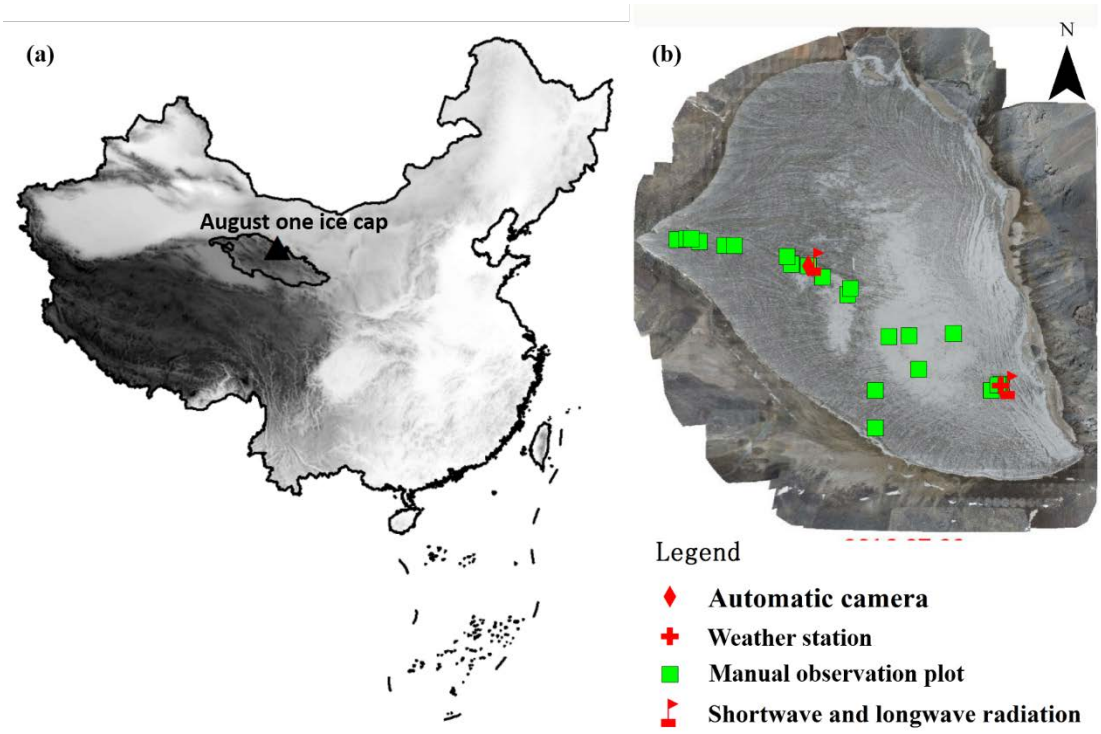
(a)
August one ice cap
(b)
N
Legend
Automatic camera
Weather station
Manual observation plot
Shortwave and longwave radiation

695

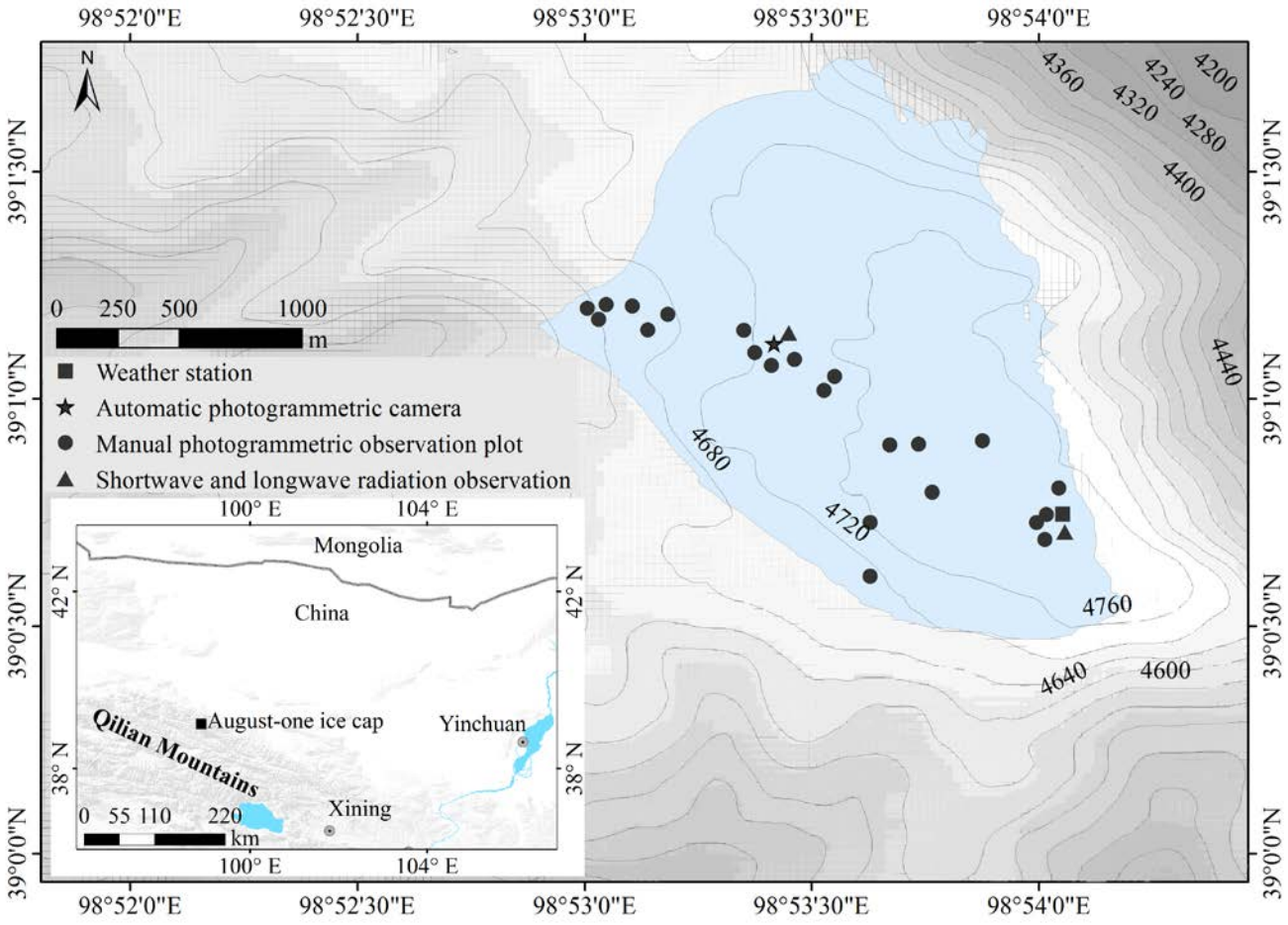

Figure 1. Location of ice cap and study sites. (a) Location of the August-one glacier, (b) Locations of the AWS, automatic and manual photogrammetry plots, and shortwave observation platforms.

Researchers had access to meteorological data that had been recorded continuously since September 2015, when an automatic weather station (AWS) was sited at the top of the ice cap (Table 1). The AWS measures air temperature, relative humidity, and wind speed at 2 and 4 m above the surface. Air pressure, incoming and reflected solar radiation, incoming and outgoing long wave radiation, glacial surface temperature (using an infrared thermometer) are measured at 2 m height. Mass balance is measured by a Campbell Scientific ultrasonic depth gauge (UDG) close to the AWS. An all-weather precipitation gauge adjacent to the AWS measures solid and liquid precipitation~~. An all-weather precipitation gauge with a windbreak fence has been installed about 2 m away from the station~~. All sensors sample data every 15 seconds. Half-hourly means are stored on a data logger (CR1000, Campbell, USA). Throughout the entire melting season (from June to September) researchers periodically checked the AWS station, to make sure that it remained horizontal and in good working order. During the entire study period, precipitation total was 261.3mm as measured at the AWS. Of that, 172.1 mm was snow or sleet and 89.2 mm was rainfall (Figure. 7 a).

Table 1 Measurement specifications for the AWS located at the top of the glacier (4820 m a.s.l.). The heights indicate the initial sensor distances to the glacier surface; the actual distances derived from the SR50A sensor.

Variable	Sensors	Stated accuracy	Initial Height (m)
Air temperature	Vaisala HMP 155A	± 0.2ºC	2, 4
Relative humidity	Vaisala HMP 155A	± 2%	2, 4
Wind speed	Young 05103	± 0.3 m/s	2, 4
Wind direction	Young 05103	± 0.3º	2, 4
Ice temperature	Apogee SI-11	± 0.2ºC	2
Shortwave radiations	Kipp&Zonen CNR-4	± 10% day total	2
Longwave radiation	Kipp&Zonen CNR-4	± 10% day total	2
Surface elevation changes	Campbell SR50A	± 0.01 m	2
Precipitation	OTT Pluvio^2	± 0.1 mm	1.7

2.2 Automatic photogrammetry

The study began with the placement of an automatic close range photogrammetry measurement apparatus in the middle of the ice cap (4700m (98º 53.4′ E, 39º 1.1′ N. See Figure 1b and Figure2~~a~~). It was placed near the existing meteorological station. This was done on July 10, 2018. A wooden frame, 1.5 m wide, and 2 m long, was put on the ice surface. This frame served as a geo-reference control field (Figure. ~~2b~~3a). Four feature points demarcated the control field; three additional points served as check points. A Canon EOS 1300D cameras with an image size of 5184×3456 pixels was connected to the frame. The camera lens was set in wide-angle mode (focal length of 27mm). The f-stop was fixed at f 25 with an exposure time of 1/320s. The camera was programmed to automatically take seven pictures over a period of ten minutes. The photography was repeated at three-hour intervals from 9:00 AM to 18:00 AM, Beijing time. During the ten-minute photography periods, the camera moved along a 1.5 m long slider rail. The camera was 1.7m above ice surface and moved along the control frame. The seven pictures taken during this period were merged to produce a picture of ice surface topography at millimeter scale (Figure ~~2~~3b). This apparatus took pictures over a period of three months (July 12 to September 15, the melting season). Sixty-~~three~~four days of data were recorded. Each daily photography series produced four sets of pictures (twelve hours, three hour intervals). The best-exposed photo sets were manually selected and used as that day's data. We also set up instrumentation to record incoming and reflected solar radiation. Samples were taken every 15 seconds; 10-minute means were stored on a data logger (CR800, Campbell, USA) located at a height of 1.5m. Surface elevation changes caused by accumulation and ablation was measured by a~~Mass balance was measured by~~ digital infrared hunting-video camera, which took pictures of ice-surface gauge stakes located near the automatic photogrammetry site.

2.3 Manual photogrammetry

Manual close-range photogrammetry was used to survey glacier surfaces at several different locations of the ice cap. Observations were made on four days: July 12 and 25, and later on August 3 and 28. It should be noted that when the July measurements were performed, the ice cap surface was partially snow-covered.

Channels account for only a small portion of the glacier surface area. These surfaces show extreme variability of z_0 (Rippin et al., 2015; Smith et al., 2016). For that reason, we distributed the manual photogrammetry study sites over the glacier surface in such a way as to cover most surface types and topographic regions without including any channels ~~f~~(Figure 1b). We photographed a total of thirty-six sites over the four days of observation.

Study plots were demarcated with a 1.1×1.1m portable square aluminum frame. Geo-reference of the point cloud was enabled using control points established by eight cross-shaped screws on the aluminum frame (Figure.~~2c~~3c). Photos ~~pairs~~ (convergent photographs, low oblique photos in which camera axes converge toward one another) were taken at ~1.6 m distances, covering an area of ~1.75 m^2. Seven to twelve of such photos were taken at each survey site and surrounded the target area from different directions. The camera used was an EOS 6D 50mm, with fixed focal lens and an image size of 5472×3648 pixels. The f-stop was fixed at f 22 with an exposure time from 1/25 to 1/125 s.

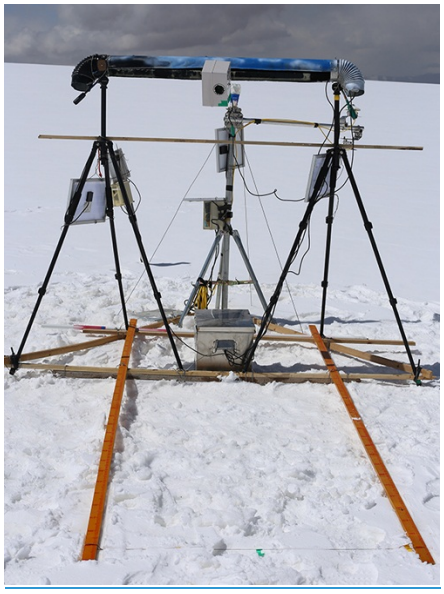

Figure 2 The automatic photogrammetry device at the August-one ice cap.

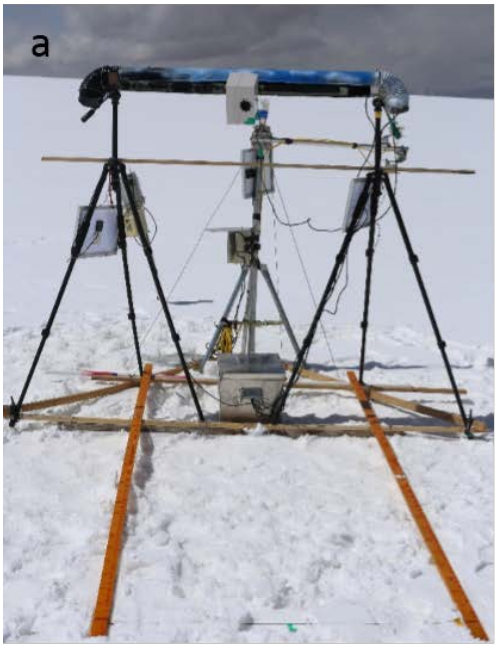

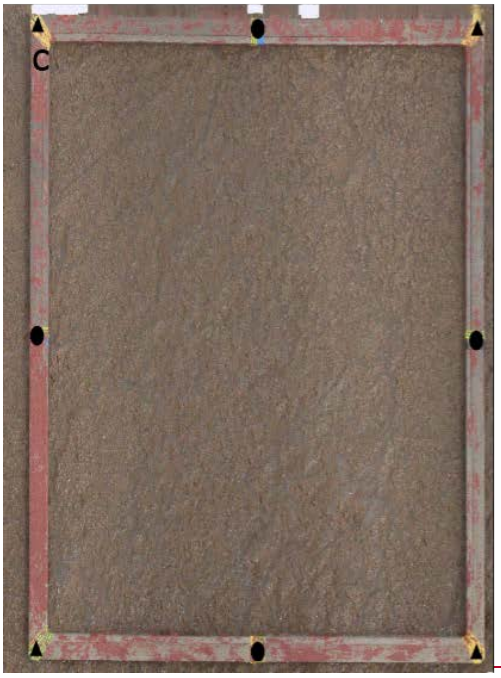

Legend

▲ **Control points**

● **Check points**

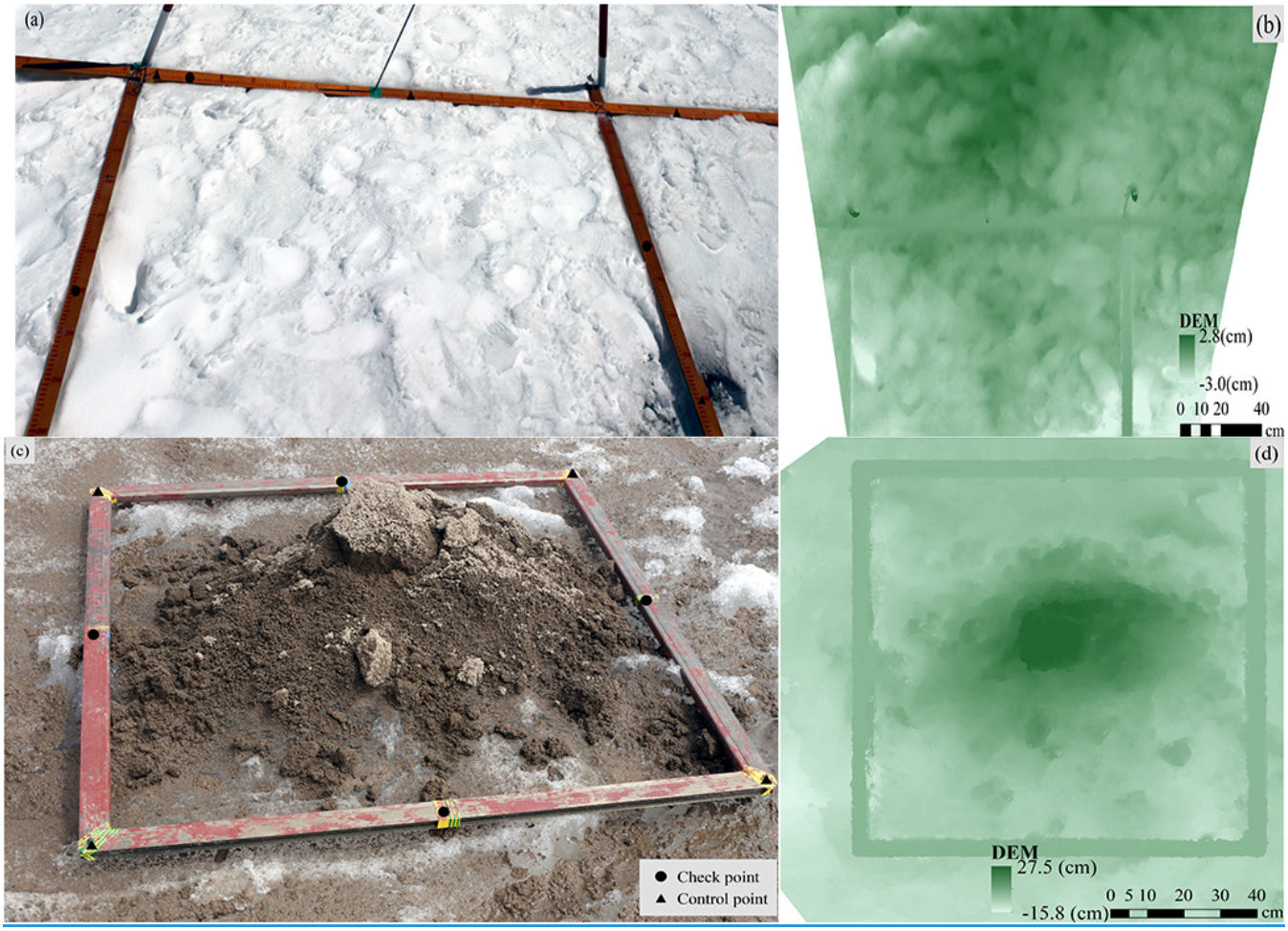

Figure 3. Frames used for automatic and manual photogrammetry. (a) Wooden frame in situ applied in automatic photogrammetry, four control points and three check points are shown on the frame; (b) Detrended DEM for the corresponding snow surface of Figure3a; (c) Manual observation plot, four control points and four check points shown on the aluminum frame. Ice surface hummocky was covered with cryoconites. (d) Detrended DEM for the corresponding cryoconites surface of Figure 3c.

~~Figure 2. Frames used for automatic and manual photogrammetry. (a) The automatic photogrammetry device applied in the observation of ice surface roughness in the August one ice cap. (b) Aluminum frame in situ; ice surface was covered with cryoconite. Four control points and three check points are shown on frame. (c) Manual observation plot; dense point cloud viewed from above; ice surface was covered with cryoconite. Four control points and four check points shown on wooden frame.~~

2.4 Data processing

Structure-from-motion photogrammetry is revolutionizing the collection of detailed topographic data (Westoby et al., 2012; James et al., 2017). High resolution DEMs produced from photographs acquired with consumer cameras need careful handling (James and Robson, 2014). In this study, b~~B~~oth manual and automatically derived photographs were imported into a software program, Agisoft Photoscan Professional 1.4.0. This software allowed us to estimate camera intrinsic parameters, camera positions, and scene geometry. Agisoft Photoscan Professional is a commercial package which implements all stages of photogrammetric processing (James et al., 2017). ~~.~~ It has previously been used to generate three-dimensional point clouds and digital elevation models of debris-covered glaciers (Miles et al., 2017; Quincey et al., 2017; Steiner et al., 2019), ice surfaces and braided meltwater rivers (Javernick et al., 2014; Smith et al., 2016).~~of ice surfaces and braided meltwater rivers (Javernick et al., 2014;Smith et al., 2016).~~ In our study, we found that after new snowfall, it was difficult to match feature points in the photo sets. Three days of automatic data could not be processed. We estimated z_0 data for the missing days based on data from snowfall days at the automatic site.

~~After new snowfall, it was difficult to match feature points in the photo sets. Three days of automatic data could not be processed. We estimated z_0 data for the missing days based on data from snowfall days at the automatic site.~~

2.5 Aerodynamic ~~R~~roughness ~~calculation~~estimation

Methods for measuring roughness at plot-scale were first developed by soil scientists (Dong et al., 1992; Smith, 2014). Metrics such as the random roughness (RR) or root mean square height deviation (σ), the sum of the absolute slopes (ΣS), the microrelief index (MI), and the peak frequency (the number of elevation peaks per unit transect length) were used. Later these roughness indices were used to describe snow or ice surface roughness (Rees and Arnold, 2006; Fassnacht et al., 2009b; Irvine-Fynn et al., 2014).

Current photogrammetry methods produce high-resolution three-dimensional topographic data. Earlier two-dimensional profile-based methods for estimating surface roughness discard much of the potentially useful three-dimensional topographic data (Passalacqua et al., 2015)~~(Passalacqua et al. 2015)~~. Smith et al. (2016) were able to use equation (1), developed by Lettau (1969), to make better use of the topographic data, using multiple point clouds and digital elevation models (DEM). Fitzpatrick et al. (2019) also developed two methods for the remote estimation of z_0 by utilizing lidar-derived DEM.

In this method, z_0 is quantified as:

$$z_0 = 0.5h^* \frac{s}{S} \qquad (1)$$

where: h^* represents the effective obstacle height (m) and is calculated as the average vertical extent of micro-topographic variations; s is the silhouette area facing upwind (m^2); S is the unit ground area occupied by micro-topographic obstacles (m^2); and 0.5 is an averaged drag coefficient.

Based on the work of Lettau (1969), Munro (1989) simplified the equation (1)~~A profile-based roughness measure can be calculated based on a simplified Lettau equation (see 1 above)~~ by assuming that h* can equal twice the standard deviation of

elevations in the de-trended profile, with the profile's mean elevation set to 0 meter. The aerodynamic roughness length for a given profile then becomes

$$z_0 = \frac{f}{X}(\sigma_d)^2 \quad (2)$$

~~$z_t = \frac{f}{X}(\sigma_t)^2$ (2)~~

Where f is the number of up-crossings above the mean elevation in profile; X is the length (m) of profile, and σ_d is the standard derivation of elevations of profile.

For manual photogrammetry, we put the aluminum frame horizontally over the ice surface, the plot is detrended by setting the control points at z axis of the same values. For automatic photogrammetry, the control field of wooden frame was also laid horizontally over the ice surface that lowered as the ice melted and maintained a horizontal position between the control field and ice surface. A DEM based approach enables the roughness frontal area s to be calculated directly for each cardinal wind direction (Smith et al., 2016). The combined roughness frontal area was calculated across the plot, the ground area occupied by micro-topographic obstacles is $1m^2$. We used a DEM-based average ($\bar{z}_{0\_DEM}$) of four cardinal wind directions to represent overall aerodynamic surface roughness. Based on the half-hour wind direction data at the August-one ice cap, the daily upward wind direction DEM-based z_{0_DEM} was also estimated at the automatic photogrammetry site. Considering that wind direction changed during the day, in this case we selected the prevailing wind direction to calculate frontal area s. The prevailing upwind direction DEM-based z_{0_DEM} was applied to calculate turbulent heat flux. Using the Munro (1989) method, $z_{0\_Profile}$ was calculated for every profile (n=1000) in both orthogonal directions for each plot at the automatic photogrammetry site.

~~Smith et al. (2016) found that there was little difference between the DEM-based z_0 values and values calculated from profiles if the results were averaged over all cardinal wind directions. In this study, we used a DEM-based average z_0 of four cardinal wind directions to represent overall surface roughness.~~

2.6 Snow and ice surface energy balance calculation

The temporal variation of z_0 at the automatic site was studied from energy balance perspective. The surface heat balance of a melting glacier is given by:

$$Q_M = Q_{is} - Q_{os} + Q_L + Q_E + Q_H + Q_P + Q_G \quad (3)$$

Where, Q_M is the heat flux of melting; Q_{is} is the incoming shortwave radiation; Q_{os} is the outgoing shortwave radiation; Q_L is the net longwave radiation; Q_E is the latent heat flux; Q_H is the sensible heat flux; Q_P is the heat from rain; and Q_G is subsurface heat flux.

In a horizontally homogeneous and steady surface state, the surface heat fluxes Q_E and Q_H can be calculated using either the bulk aerodynamic approach or profile method, based on the Monin-Obukhov similarity theory (e.g., ; Arck and Scherer, 2002; Garratt, 1992; Oke, 1987). In this study, half-hour observations at 4 m level and daily upward wind direction DEM-based z_0 were used to calculate Q_E and Q_H based on the bulk method. The heat from rain is given by Konya and Matsumoto (2010):

$$Q_P = \rho_w C_W T_W P_r \quad (4)$$

Where, ρ_w is the density of water(1000 kg m^{-3}); C_W is the specific heat of water (4187.6 J kg^{-1} K^{-1}); T_W is the wet-bulb temperature (K); and P_r is the rainfall intensity (mm). The subsurface heat flux Q_G is estimated from the from the temperature-depth profile and is given by $Q_G = -k_T \frac{\partial t'}{\partial z'}$ where k_T is the thermal conductivity, 0.4Wm^{-1}K^{-1} for old snow and 2.2W m^{-1}K^{-1} for pure ice (Oke, 1987).

In order to calculate P_r, we used the air temperatures recorded at the AWS. There is an elevation difference between the study site (4700 m) and the AWS (4790m); recorded air temperatures were corrected to account for the elevation difference, a lapse rate of -5.6 ^{o}C Km^{-1} was applied based on observation nearby (Chen et al., 2014) . The ice cap is flat and open terrain so in this case wind speed and relative humidity at the study sites were assumed to be close to those observed at the AWS.~~recorded air temperatures were corrected to account for the elevation difference, assuming a lapse rate of -7 ℃ Km^{-1}. Wind speed and relative humidity at the study sites were assumed to be equal to those observed at the AWS, as measurements taken by the AWS are broadly representative of the whole ice cap.~~

3. Results

3.1 Photogrammetry precision

We used seventeen plots~~control points and check points~~ to analyze the horizontal and vertical accuracy of our automatic photogrammetry, and thirty-one plots~~pairs~~ for our manual photogrammetry. Based on the Agisoft PhotoScan processing report, automatic photogrammetry average point density of the final plot point clouds was over ~~Automatic photogrammetry: average point density of the final plot point clouds was >~~1,000,000 points m^{-2}. DEMs of ~~0.~~1mm resolution were generated at plot scale. The average geo-reference errors fluctuated around~~were less than~~ 1 millimeter (see Tables ~~1~~2 and ~~2~~3). Total RMSE of the automatic control points was 3.0±2.1 mm, for check points 3.62±1.6 mm. Vertical error for control points was 3.58mm±3.01mm, and 4.83~~mm~~ ±2.9mm for check points (Tables ~~1~~2 and ~~2~~3). Standard deviation of c~~C~~ontrol and check point errors are all within 15 ~~cm~~mm (Figure 4a, 4c, 4e). Manual measurements~~:~~ average point density of the final plot point clouds was >6,000,000 points m^{-2}. DEM of ~~0.~~1 mm resolution was generated at plot scale. Root mean square error (RMSE) of 4 control points is 1.78±1.3 mm (Table 1). Control points vertical accuracy of manual photogrammetry is about 1.65±1.3 mm. Total RMSE of manual photogrammetry check points is 0.99±0.3 mm, vertical accuracy is 0.66±0.3mm (see Tables ~~1~~2 and ~~2~~3). Standard deviation for x, y and z axis were all within 5mm (Figure 4 b, 4d, 4f).

Table ~~1~~2 Control point RMSE for manual and automatic photogrammetry

	Ground control points	X error (mm)	Y error (mm)	Z error (mm)	Total error (mm)
Automat	Point 1	0.71	5.83	6.61	5.11
	Point 2	0.41	1.14	0.74	0.82
	Point 3	0.54	4.55	2.40	2.99

	Point 4	0.45	0.76	1.04	0.79
	Average	**0.54**	**3.76**	**3.58**	**3.01**
Manual	Point 2	0.62	0.43	0.81	1.11
	Point 4	0.44	0.27	0.43	0.67
	Point 5	0.18	0.47	0.85	0.99
	Point 7	0.66	0.39	2.97	3.07
	Average	**0.52**	**0.40**	**1.65**	**1.78**

Table ~~2~~ 3 Check point RMSE for manual and automatic photogrammetry

	Ground Check points	X error (mm)	Y error (mm)	Z error (mm)	Total error (mm)
Automatic	Point 5	2.06	4.44	7.70	5.27
	Point 6	0.91	3.56	1.95	2.40
	Point 7	0.98	3.11	2.60	2.41
	Average	**1.41**	**3.74**	**4.83**	**3.62**
Manual	Point 1	0.30	0.19	0.39	0.52
	Point 3	0.79	0.37	0.69	1.12
	Point 6	0.28	0.83	0.90	1.26
	Point8	0.46	0.45	0.44	0.77
	Average	**0.52**	**0.53**	**0.66**	**0.99**

Note that the control and check point errors are larger for the automatic measurements than for the manual ones (See Figures 4). We believe that this is the case because, rather than using static f-stop and exposure times (as in automatic photogrammetry) researchers engaged in manual photogrammetry could adjust exposure time based on ice surface conditions. This allowed production of better quality photos even on cloudy or foggy days. ~~(See Figures 3 and 4).~~ The difference of survey design also caused more precise results for manual than automatic photogrammetry. For the automatic measurements, the camera was moving linearly, and the density of tie-points was much higher in the foreground compared to the background. For the manual method, photos were taken by surrounding the target area. This type of surface provided a much more robust elevation model and points density. ~~However, even automatic measurements satisfied the requirement outlined by Rees and Arnold (2006) that millimeter vertical accuracy was required and would suffice to calculate surface roughness (z_0).~~

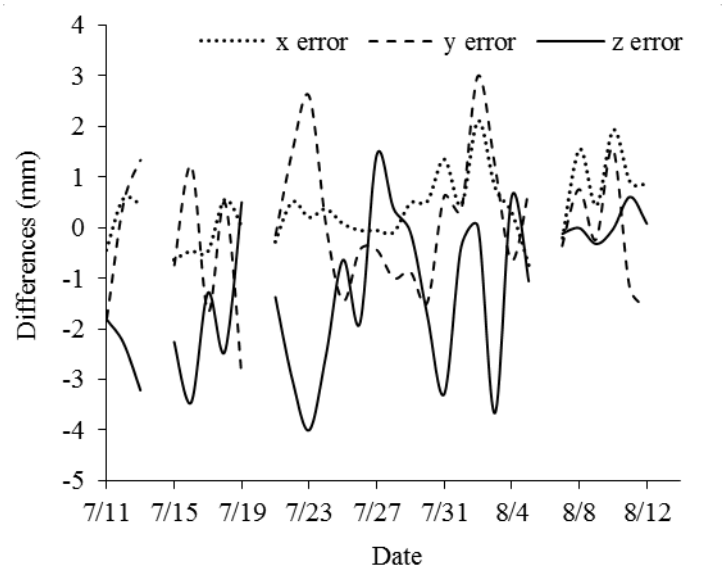

~~Figure 3. Automatic photogrammetry checkpoint errors~~

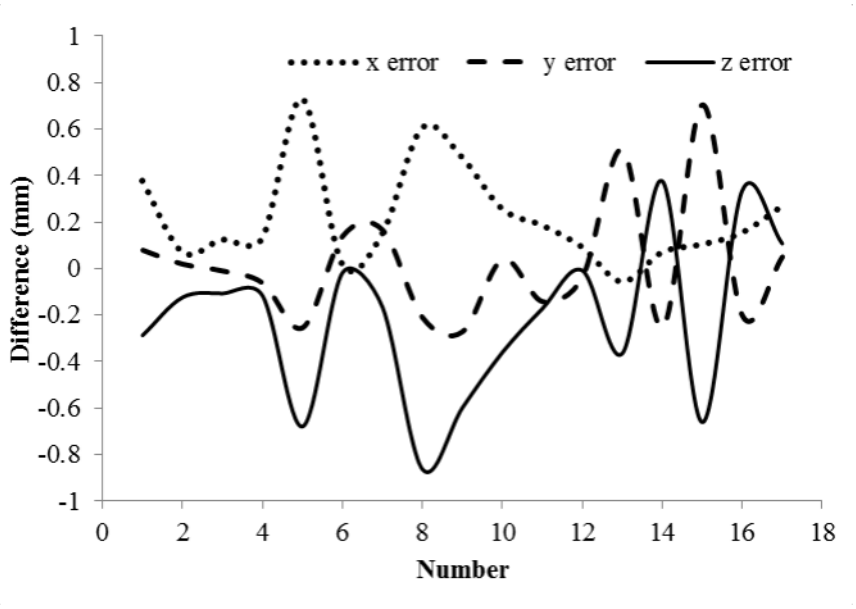
x error
y error
z error
Difference (mm)
Number
1
0.8
0.6
0.4
0.2
0
-0.2
-0.4
-0.6
-0.8
-1
0
2
4
6
8
10
12
14
16
18

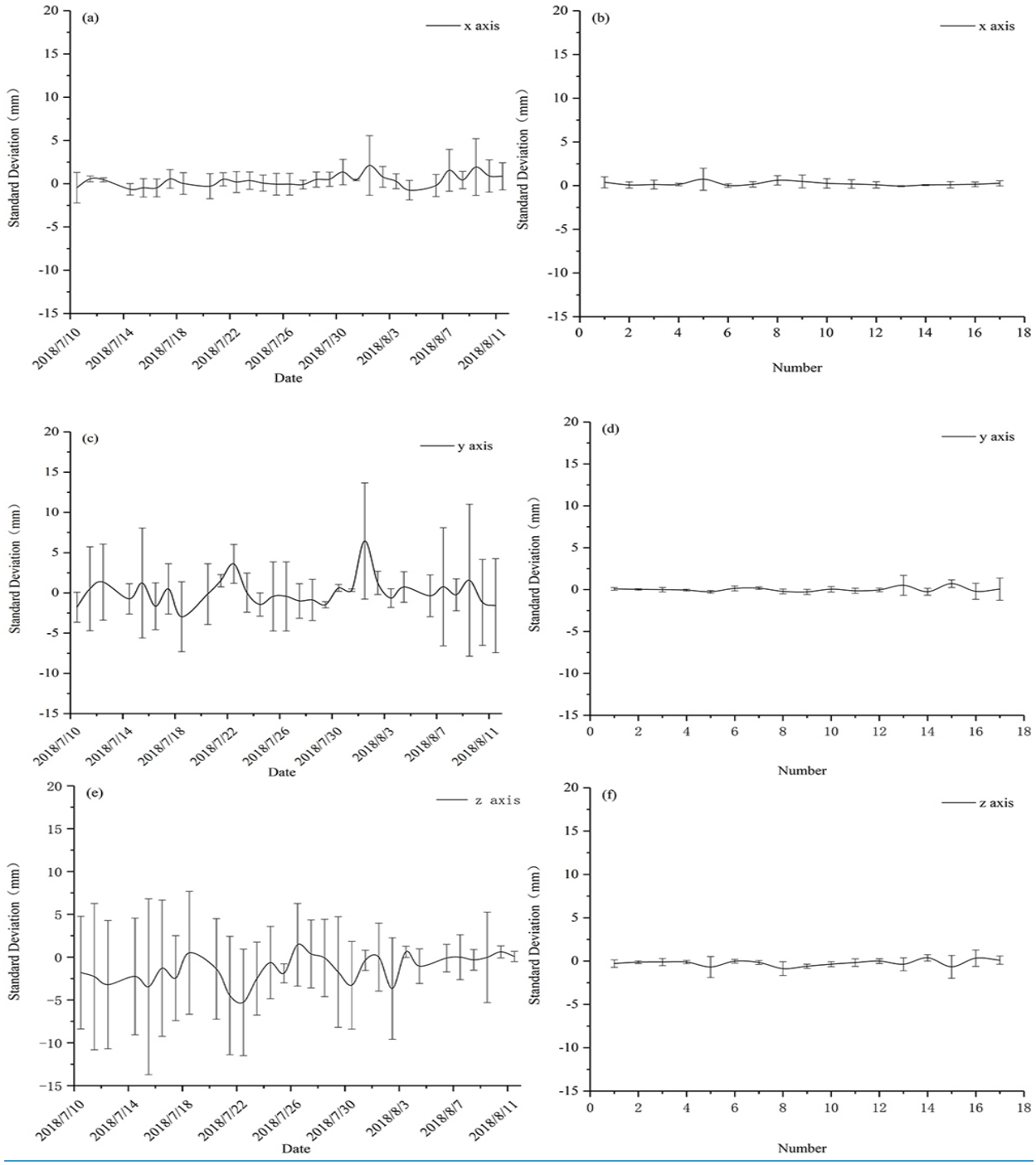

885 **Figure 4. Automatic and manual photogrammetry checkpoint errors. (a), (c) and (e) are automatic photogrammetry standard deviation for x, y and z axis. (b), (d), and (f) are manual photogrammetry standard deviation for x, y and z axis.** ~~**Figure 4. Manual photogrammetry checkpoint errors**~~

3.2 Aerodynamic ~~S~~surface roughness as measured by automatic photogrammetry

Data for ice surface roughness was collected by the automatic photogrammetry camera site from July 12 to September 15, a period covered the whole melting season. Profile and DEM data show that z_0 estimates vary by two orders of magnitude over the study period (Figure 5)~~was highly variable over the study period (Figure 5)~~. The upwind DEM-based data showed a z_{0_DEM} varying from 0.1 mm to 1.99mm (mean: 0.55 mm). The average of four cardinal wind directions DEM data shows a $\bar{z}_{0\_DEM}$ varying from 0.1mm to 2.55 mm (mean: 0.57 mm). The average Munro profile based $z_{0\_Profile}$ varied from 0.03mm to 2.74 mm (mean 0.46 mm).~~The profile data shows a z_0 varying from 0.05 mm to 2.74mm (mean: 0.45 mm). The DEM data shows a z_0 varying from 0.02mm to 2.56 mm (mean: 0.51 mm).~~

At the start of the observation period of July 12, snow covered the study site. As the snow melted, the ice cap ~~glacier~~ surface z_0 increased. During this periods, z_0 dropped to around 0.1mm due to intermittent snowfall. ~~(save during periods of intermittent snowfall, when z_0 dropped to ~0.1mm).~~ On July 21, cryoconites appeared on patches of snow-crust, which led to patchy melt. From July 21 to 24, overall $\bar{z}_{0\_DEM}$~~z_0~~ increased from 0.1mm to 1.6mm. By July 29, snow had disappeared from the study site; z_0 fluctuated but trended lower. From July 29 to August 5 bare ice covered whole field of view; $\bar{z}_{0\_DEM}$~~z_0~~ ranged from 0.18 to 0.56mm. From August 6 to September 3 there was intermittent snowfall followed by melting; $\bar{z}_{0\_DEM}$~~z_0~~ ranged from 0.1 to 1.0mm. From September 4 to September 14 $\bar{z}_{0\_DEM}$~~z_0~~ showed an overall increase, reaching a maximum of 2.55 mm on September 8. There was intermittent snowfall during this period, which temporarily reduced $\bar{z}_{0\_DEM}$~~z_0~~. $\bar{z}_{0\_DEM}$~~Z_0~~ which then increased thanks to patchy micro-scale melting. After September 14, snow covered the whole surface of the glacier.~~—~~ and t~~T~~here was no melting and little fluctuation in z_0.

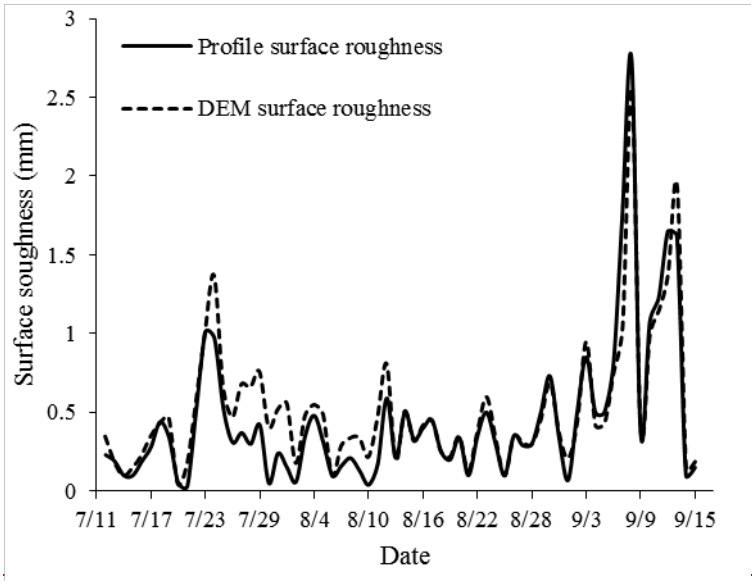

~~**Figure 5. Variation of ice surface roughness over time, automatic observation site**~~

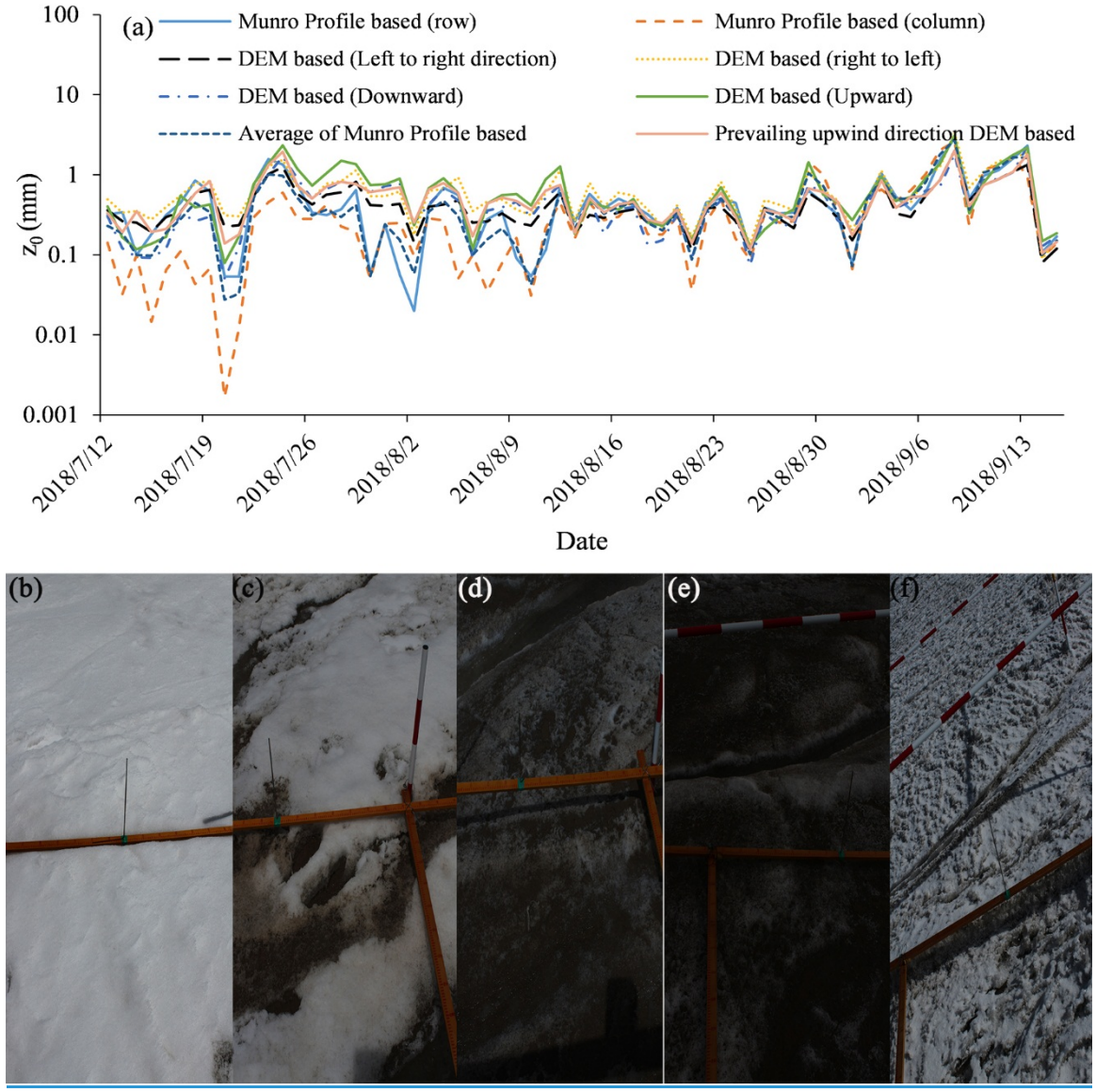

Figure 5. (a) variation of glacier surface aerodynamic roughness over time at the automatic observation site for DEM based and Munro (1989) profile based approach; photo (b) showed snow covered surface on July 13, photo (c) showed partially snow covered surface on July 23 with cryoconite holes, (d) and (e) showed smooth ice surface on August 1 and August 30, (f) showed rough ice surface on September 13

It should be clear that either $z_{0\_Profile}$ or z_{0_DEM} and $\bar{z}_{0\_DEM}$ varied following the same pattern during the melting season. ~~z_0 varied greatly during melting season~~. There were two peaks in z_0, both of which occurred in period of transition: snow surface turning to ice around July 24 and ice surface turning to snow on September 8. On July 24 and again on September 8 and 13, glacier surfaces featured cryoconite holes and snow crust. Both the automatic and manual observations showed the same pattern: maximum z_0 at snow-ice transition belt during partially snow-covered periods.

3.3 Surface roughness as measured by manual photogrammetry

No wind direction measurements were carried out during manual photogrammetry. In this case, we presented an average of four cardinal directions to represent ice aerodynamic surface roughness. Analysis indicated that $\bar{z}_{0\_DEM}$ proved to have an interesting relationship with altitude. ~~Ice surface roughness proved to have an interesting relation with altitude and date.~~ $\bar{z}_{0\_DEM}$ ~~Z_0~~ was highest in the transition zone between snow cover and ice. This zone moved up the ice cap during the melting season. On July 12, ice surface roughness decreased from 3.2mm to 0.25mm as altitude increased (Figure. 6a, r= 0.8429, P=0.0006<0.01). Near the ice cap terminals of 4590m, the ice surface featured porous snow/ice and many cryoconite holes. As altitude increased, the number of cryoconite holes decreased and snow coverage increased. At 4700m the ice surface was predominantly snow covered, and only a few small patches were bare of snow. On July 25, ice surface roughness fluctuated between 0.27 to 0.65 mm at the ice cap terminals (4593m). At ~4700m, roughness increased to 1.85mm. Above that point, roughness gradually decreased to 0.25mm at the ice cap top, which was covered by snow (Figure 6b).

On August 3, the August-one ice cap was predominantly bare ice; there was scattered snow crust at the ice cap top. The ice surface, (terminals to top) showed a heavy deposit of cryoconite ~~(Figure 1c)~~. Potogrammetric data collected manually ~~Manual investigation~~ revealed that ice surface roughness increased with altitude (Figure. 6c, r=0.7~~, P=0.01<0.05~~). From terminals to top, z_0 varied from 0.06 mm to 2.2 mm. On August 29, the ice cap surface roughness showed no significant correlation with altitude (Figure. 6d, r=-0.03~~, P=0.9>0.5~~). $\bar{z}_{0\_DEM}$ ~~Z_0~~ varied from 0.2 mm to 0.98 mm (Figure6 d). When we compare the results of the four surveys, we see that ice surface roughness was ~~quite~~ variable. Maximum z_0 was seen at the snow and ice transition zone, where the ice surface featured both cryoconite holes and clean snow crust. Snow crust would have inhibited melting; cryoconite would have increased it. It is thus understandable that surface roughness would have been greater in such an area. Bare ice or snow cover both result in comparatively less roughness.

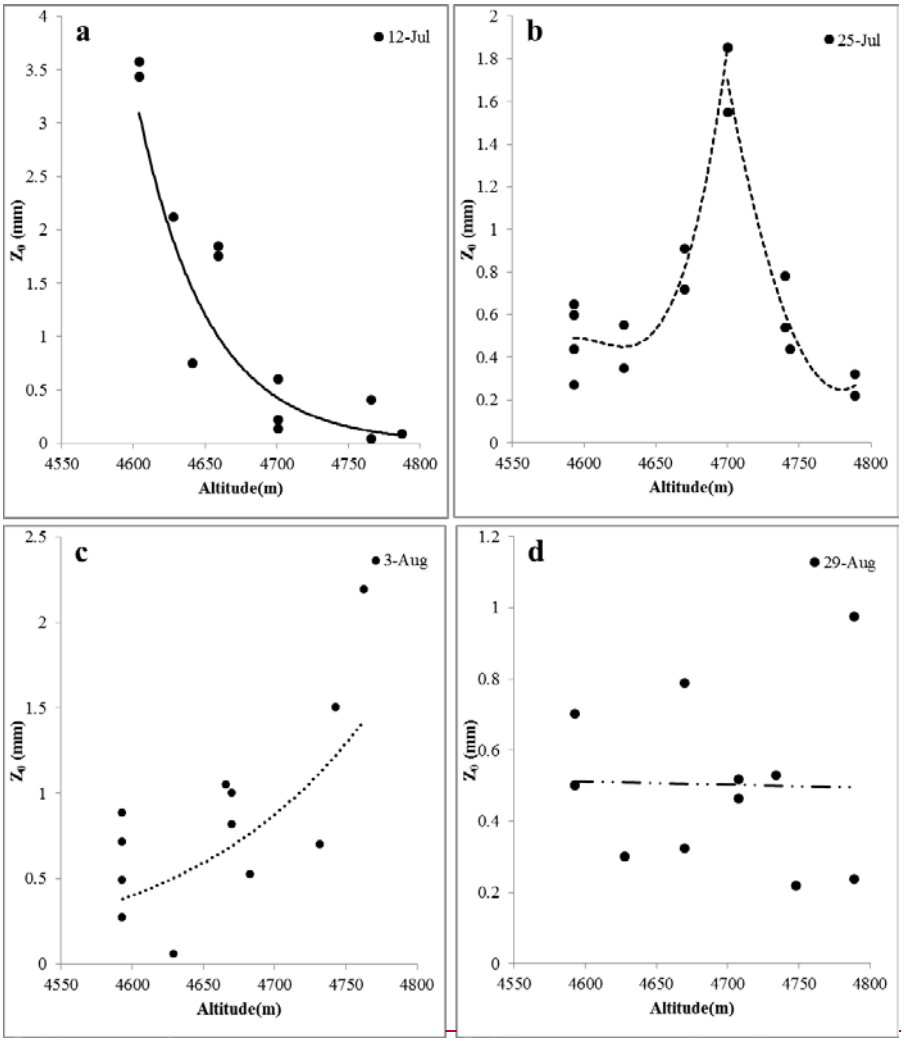
a
12-Jul
Z_0 (mm)
Altitude(m)
b
25-Jul
Z_0 (mm)
Altitude(m)
c
3-Aug
Z_0 (mm)
Altitude(m)
d
29-Aug
Z_0 (mm)
Altitude(m)

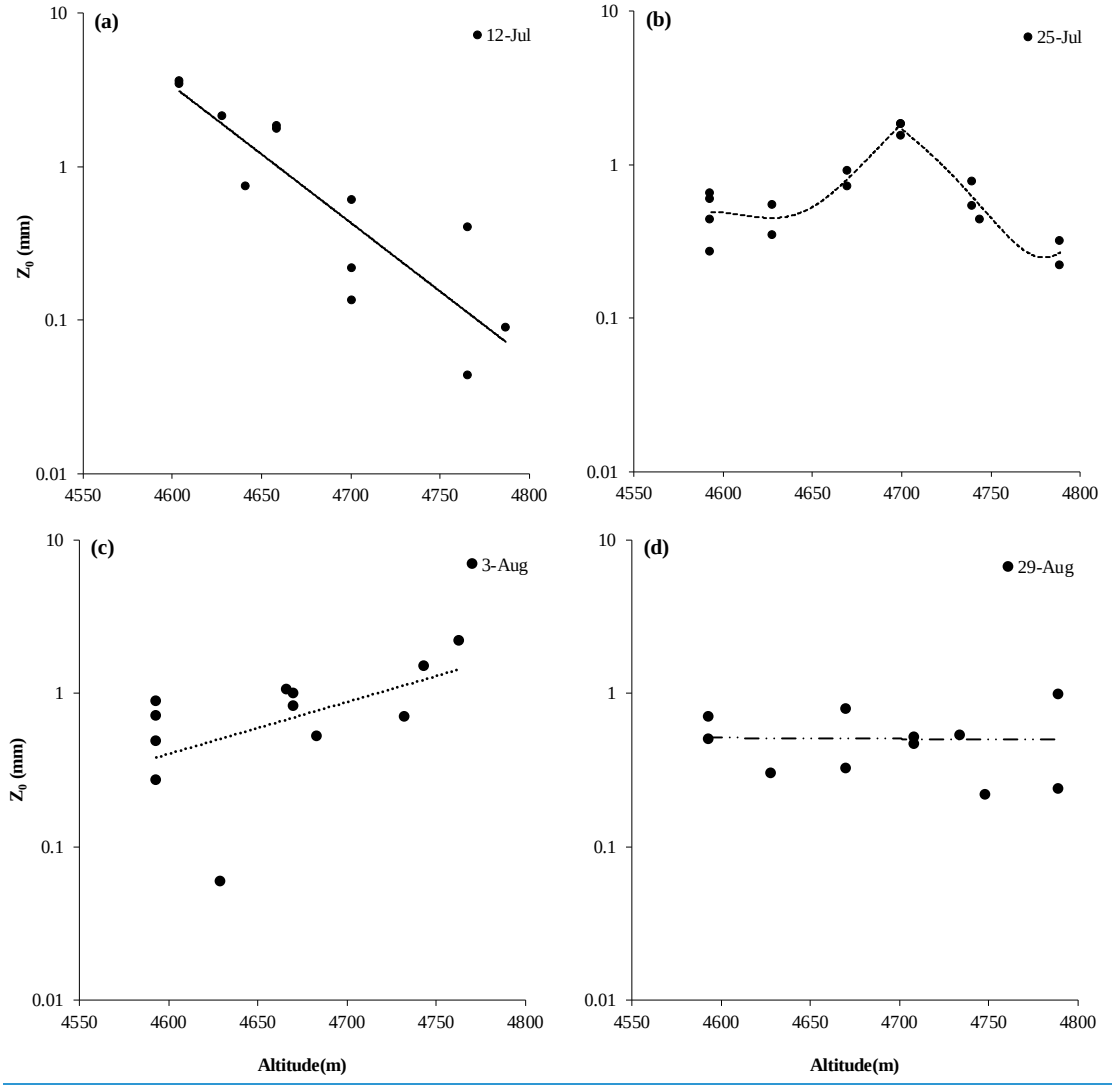

Figure 6. Surface roughness vs. altitude, (a) As observed on 12 July, (b) As observed on 25 July, (c) As observed on 3 August, (d) As observed on 28 August.

3.4 Z_0 and weather

Figure 7 compared $\bar{z}_{0\_DEM}$ and corresponding meteorological conditions of precipitation, air temperature, downward solar radiation, relative humidity and wind speed. Detailed analysis indicates ~~Snowfall~~ snowfall was recorded from July 12 to 24. In general, snowfall reduced roughness if it resulted in a fully snow-covered surface. However, if a patchy, shallow snow cover was formed, it tended to increase z_0 after a short drop. For example, on August 11 and 12, two successive sleety days created a patchy snow cover which soon increased z_0. Between July 26 and August 31 there were sixteen rainfall events, which tended to lower ice surface z_0.

Daily temperatures during the study period ranged from -6.5 °C to 7.1 °C (mean: 1.3, Figure. ~~7b~~7c). It was 1.2 °C on July 11. It increased to 3.6 °C on July 24 (the date when z_0 was highest). It continued increasing until July 29, when it reached its highest annual of 7.1 °C. During this period z_0 continuously declined. From July 28 to end of August temperatures fluctuated between -0.3 to 5.7 °C with no evident trend. $\bar{z}_{0\_DEM}$~~Z$_0$~~ also fluctuated slightly, showing no obvious trend. In September air temperature quickly dropped from 0.6 to -6.5 °C. There were large fluctuations in z_0 during this period. The largest fluctuations appeared when air temperatures dropped from positive to negative.

Daily downward mean solar radiation fluctuated dramatically during the study period due to cloud and overcast (Figure. ~~7c~~7d). Incident solar radiation fluctuated between 129W m^{-2} and 753 W m^{-2} (mean: 469 W m^{-2}). From July 29 to end of August, the weather was cloudy, warm, calm, and humid most of the time (Figure. 7b, 7c, ~~7d~~ 7e ~~7e~~7f), and $\bar{z}_{0\_DEM}$~~z$_0$~~ was relatively stable except when there was intermittent snowfall-induced fluctuation. After in September, the weather was again becoming cold and dry and z_0 was quite variable.

3.5 Ice-surface energy balance at automatic z_0 observation study site

~~Glacier surface melt and roughness are mainly governed by net shortwave and longwave radiation, sensible heat, and latent heat.~~ The following section analyzes the changes in surface energy balance at the automatic site. Meteorological observation~~Our~~ records allowed us to study the factors that control ice surface roughness. Net radiation varied from -9.7 to 260.2 W m^{-2} (mean: 95.3 W m^{-2}) during the study period. This constituted the largest energy flux affecting glacier-surface energy balance. It accounted for 84% of total incoming flux (Figure. 8). Net radiation was relatively low in the first thirteen days of the study period (mean: 69.3 Wm^{-2}), when the glacier surface was covered with snow. In the succeeding five days, net radiation increased to 103.9 W m^{-2}. At this time the ice surface exhibited a patchwork of snow, ice, and cryoconite. From July 29 to August 5 the surface of the study site was composed of ice with a dusting of cryoconite. Net radiation reached a height of 183 Wm^{-2}. There was intermittent snowfall from August 6 to September 8. Net radiation dropped to a mean 93 Wm^{-2}. Snow cover then appeared and net radiation dropped to a low of 46 Wm^{-2}.

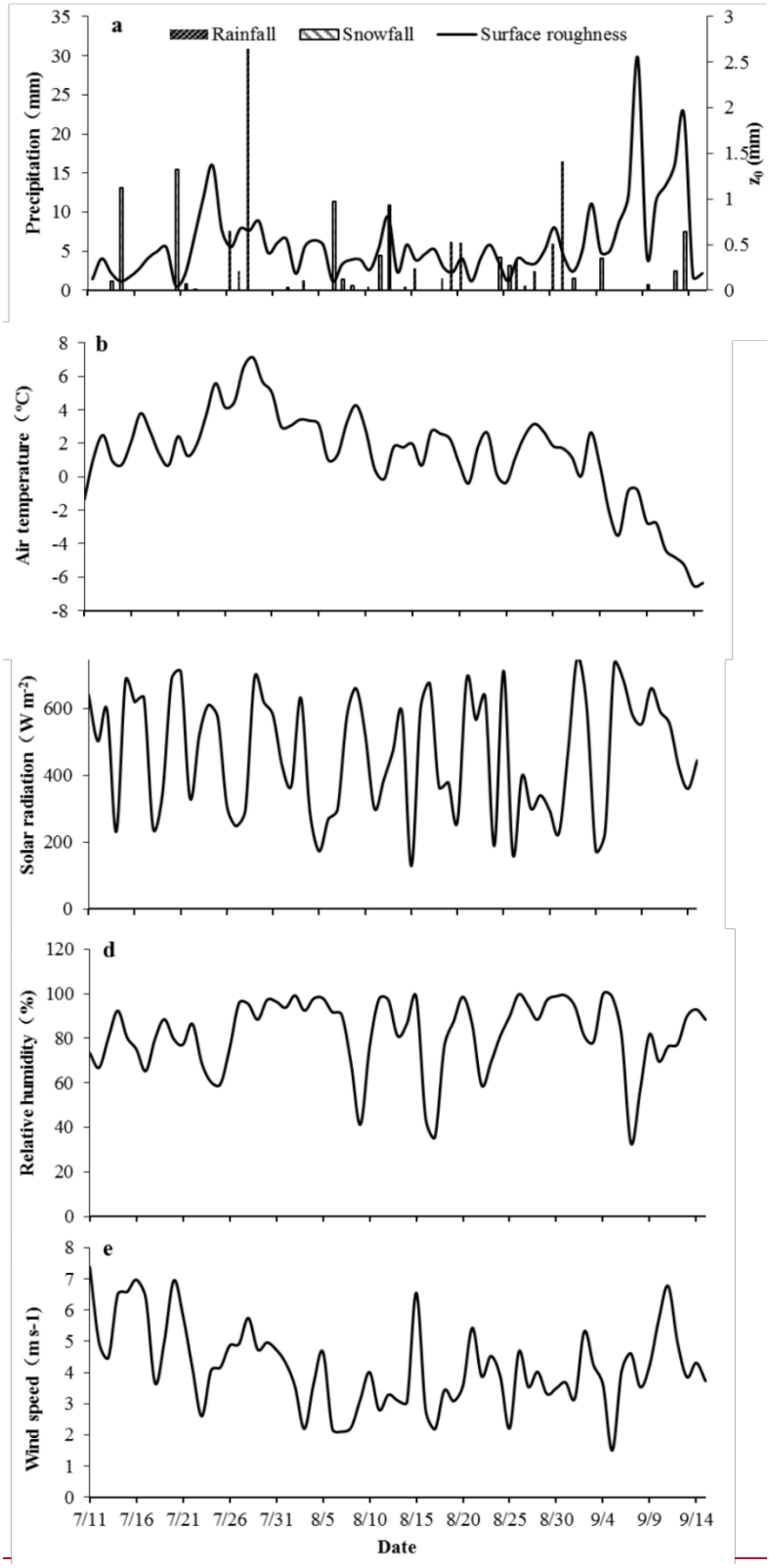
a
Rainfall
Snowfall
Surface roughness
Precipitation（mm）
z_0 (mm)
b
Air temperature（℃）
Solar radiation（W m-2）
d
Relative humidity（%）
e
Wind speed（m s-1）
7/11 7/16 7/21 7/26 7/31 8/5 8/10 8/15 8/20 8/25 8/30 9/4 9/9 9/14
Date

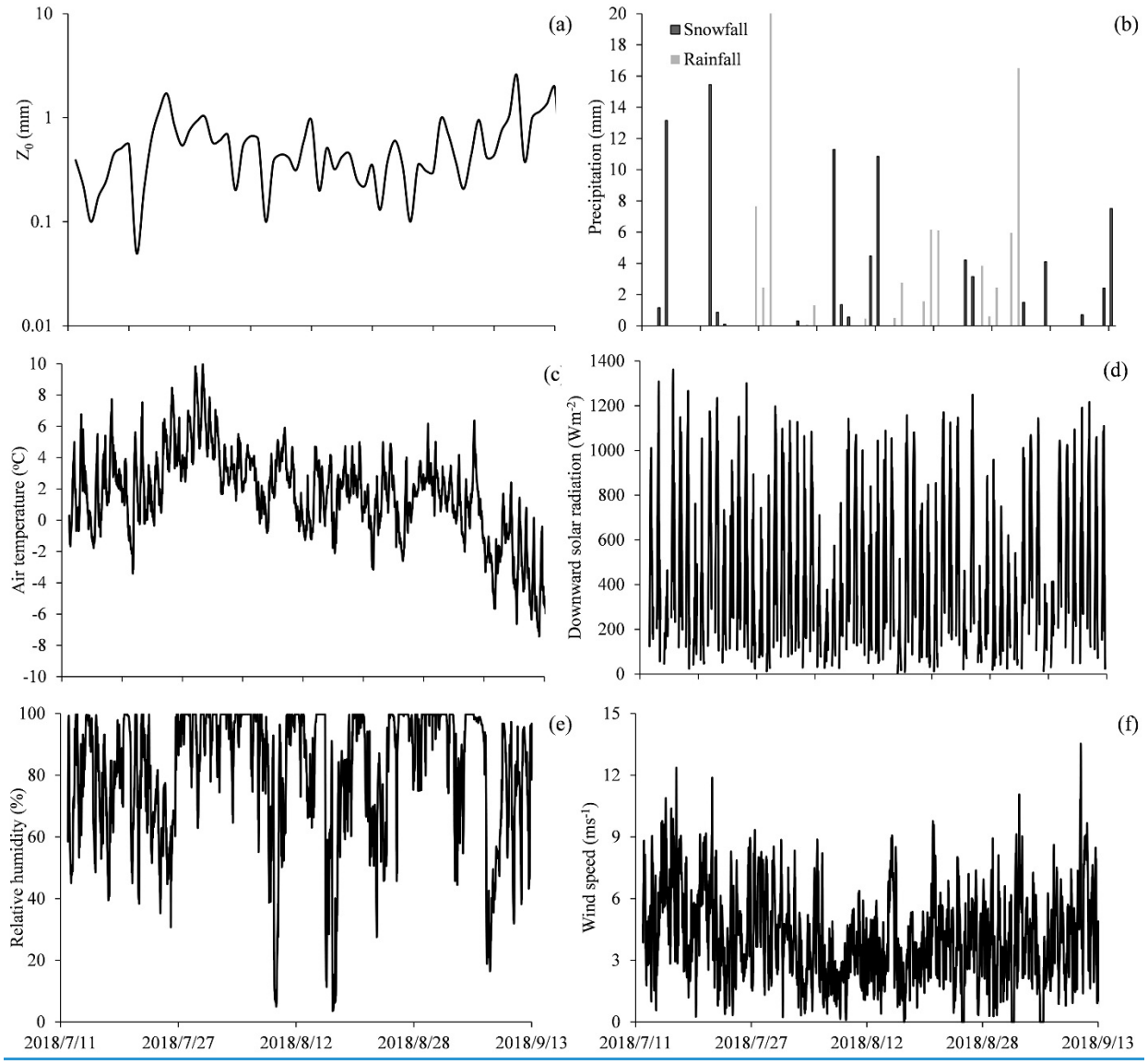

Figure 7. Weather conditions at AWS over study period. (a) Precipitation, (b) Air temperature, (c) Incident solar radiation, (d) Relative humidity, (e) Wind speed.

~~3.5.2 Sensible heat~~

Bulk method estimated results indicate that ~~S~~sensible heat (Q_H) was the second largest energy-flux component of in surface energy balance during the study period (Figure ~~7~~8). The sensible heat daily mean varied from -7.1 to 66.3 W m^{-2}. It accounted for -28% to 32% (mean: 15%) of the net energy flux. Latent heat was generally small throughout the study period. Daily mean of latent heat varied from -80.1 to 11.1 W m^{-2} (mean: -13.2 W m^{-2}). It account for a mere 0.9% for the total incoming flux. It

was negative from July 11 to 26 when the ice surface was snow covered. After July 26 the latent heat was mainly positive in the following ten days (ice surface was pure ice or partially snow covered). From August 6 to the end of the study period (September 15) it was predominantly negative.

~~3.5.4 Energy from rainfall~~

From July 25 to August 5 rainfall energy varied from 0 to 11.7 W m^{-2} (mean: 0.3W m^{-2}). Rainfall accounted for a mere 0.2% of total incoming flux. One event accounted for much of the total: on July 28 a 31mm rainfall event added a flux of 11.7 W m^{-2}, which resulted in visible smoothing of the ice surface (Figure ~~8~~9). Compared to other energy components, Q_G was very small, with a daily mean of -0.65 W m^{-2} and a maximum and minimum of -0.4 and -2.1 W m^{-2}, respectively.

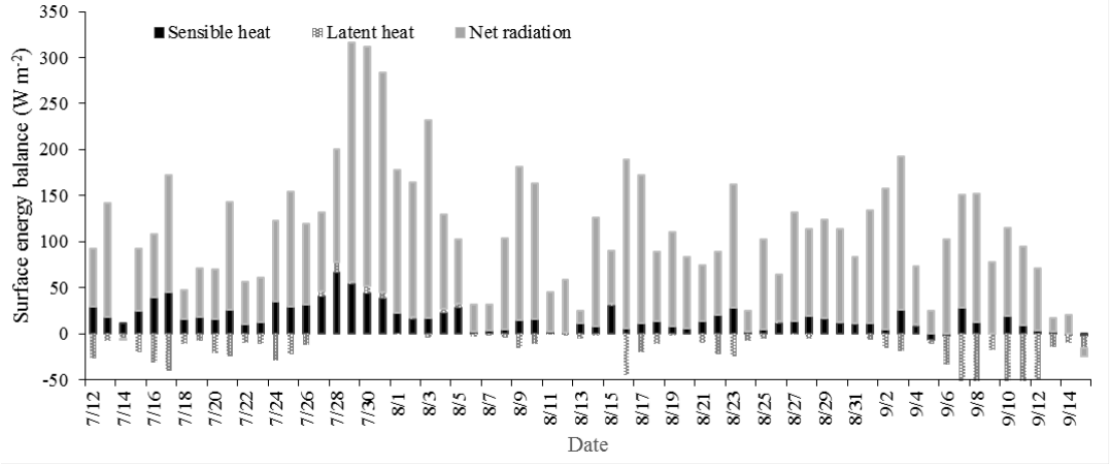

Figure 8 Daily mean of energy balance at the middle of glacier study site close to the automatic photogrammetry site.

3.5.5 Surface ablation modeled versus observed

Based on the previously listed measurements of energy fluxes we calculated the probable surface ablation at the automatic photogrammetry site. We took into account observed net radiation, bulk method calculated turbulent heat fluxes, ~~and~~ heat from rainfall, and subsurface heat flux. There was good agreement between the model and observed results (Figure ~~9~~10). ~~This suggests that our calculation of turbulent heat based on observed z_0, as entered in the model, matches the observed ablation. Such indirect observations could be useful in modeling the ablation process at other glacier study sites. We also found that the modeled mass balance did not match measurement results obtained on days with mixed snow and rain. It is likely that z_0 was more than usually variable at those times. Measurements on a finer temporal scale might be needed for calculation of turbulent heat fluxes.~~

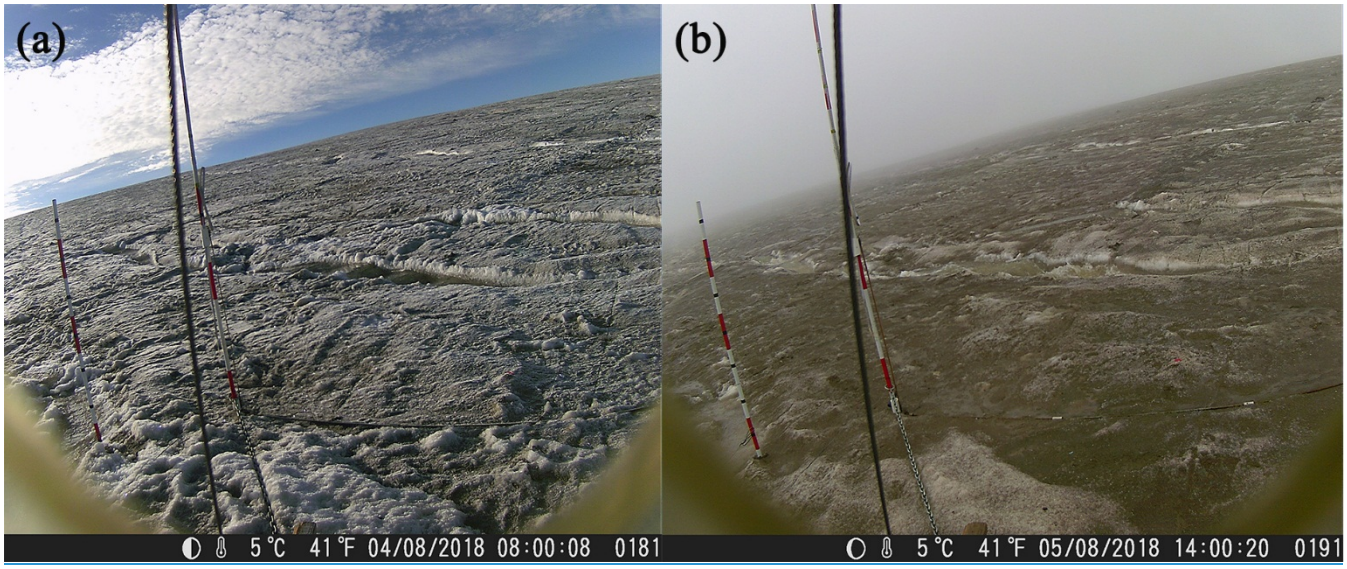

Figure 9 Ice surface overview at the automatic photogrammetry site before and after a strong rainfall event, (a) photograph before the rainfall event on August 4 of 2018, and (b) photograph after the strong rainfall event on August 5 of 2018.

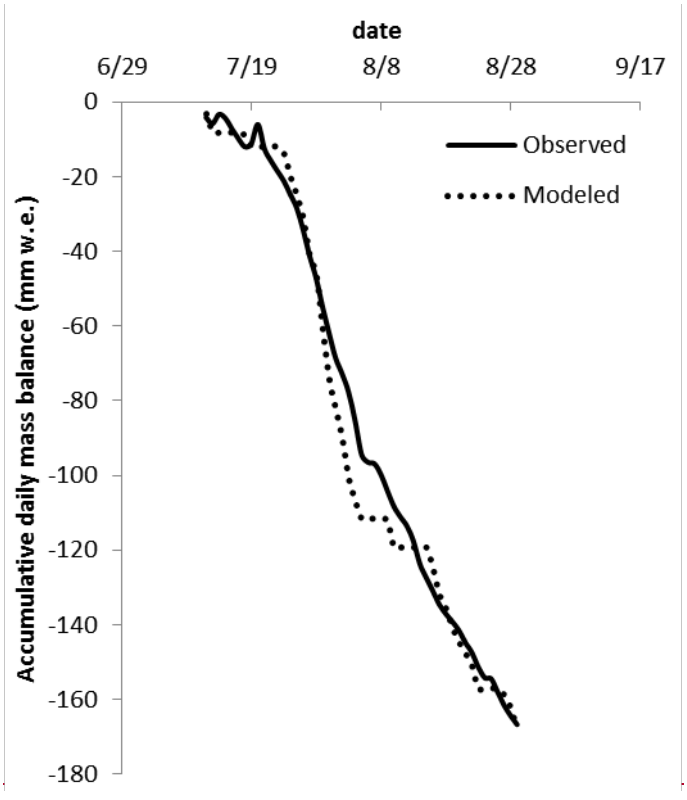

1015

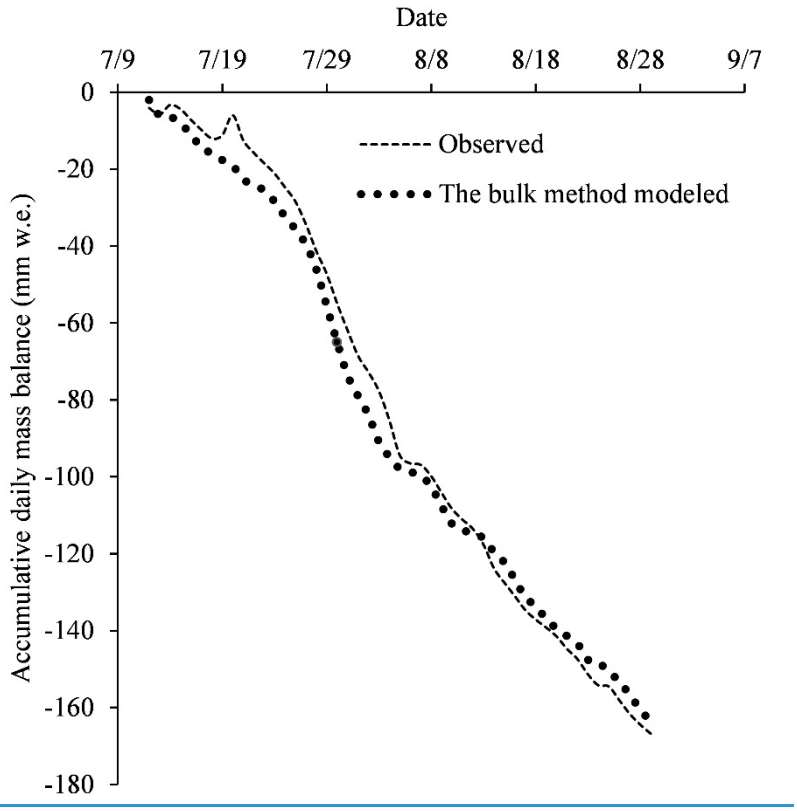

Figure ~~9~~10. Comparison of daily mass balance observed and daily mass balance as modeled. Mass balance measurements were taken from 12 July to August 29. Measurements of surface lowering were converted into water equivalents using density values.

Figure ~~10~~ 11 shows the relationship between estimated daily upward wind direction DEM-based z_{0_DEM} and the main energy flows.~~observed z_0 and the main energy flows.~~ ~~These s~~Scatter diagrams showed a positive relationship between z_{0_DEM} and net shortwave radiation (Figure 11a, r=0.1) and a significant negative relationship between z_{0_DEM} and net longwave radiation (Figure 11b, r=-0.35), Graphing z_{0_DEM} vs. bulk method estimated latent heat showed a significant negative exponential relationship (Figure 11d, r= -0.35). The scatter diagram showed no significant relationship between z_{0_DEM} and the bulk method estimated sensible heat (Figure 11c). The average of the Munro profile based $z_{0\_profile}$ and DEM based $\bar{z}_{0\_DEM}$ and the main energy items are also analyzed respectively. Scatter diagrams showed significant negative relationship between $z_{0\_profile}$ and net longwave radiation (Figure1s b, r=-0.5). Graphing $z_{0\_profile}$ vs. the bulk method estimated sensible heat showed a significant negative exponential relationship (Figure 1s d, r=-0.69). These scatter diagrams showed no significant relationship between $z_{0\_Profile}$ and the bulk method estimated sensible heat (Figure 11c, 11e). $\bar{z}_{0\_DEM}$ vs. the bulk method estimated latent heat showed a significant negative exponential relationship (Figure 2s d, r= -0.44). The scatter diagrams between $\bar{z}_{0\_DEM}$ and net shortwave radiation, the bulk method estimated sensible heat showed no significant relationship.~~no significant relationship between z_0 and net shortwave radiation, longwave radiation, and sensible heat (Figure 10a, 10b, 10c). Graphing z_0 vs. latent~~

~~heat showed a significant negative exponential relationship (Figure 9d, r= -0.61, P=0.0001<0.001). When latent heat is higher, as it is during the melting seas, z_0 decreases.~~

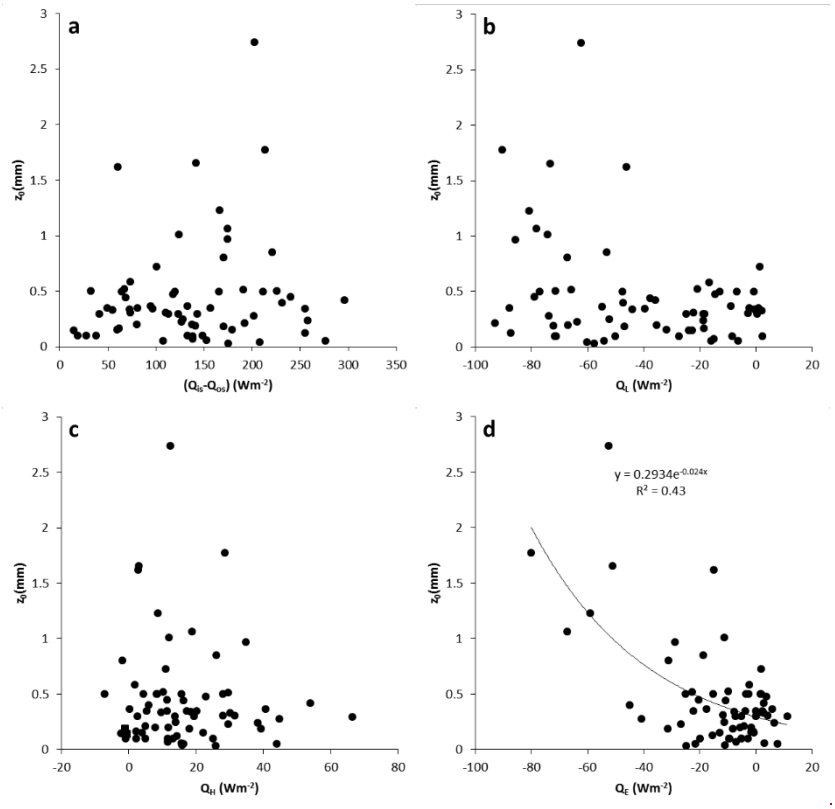

1035

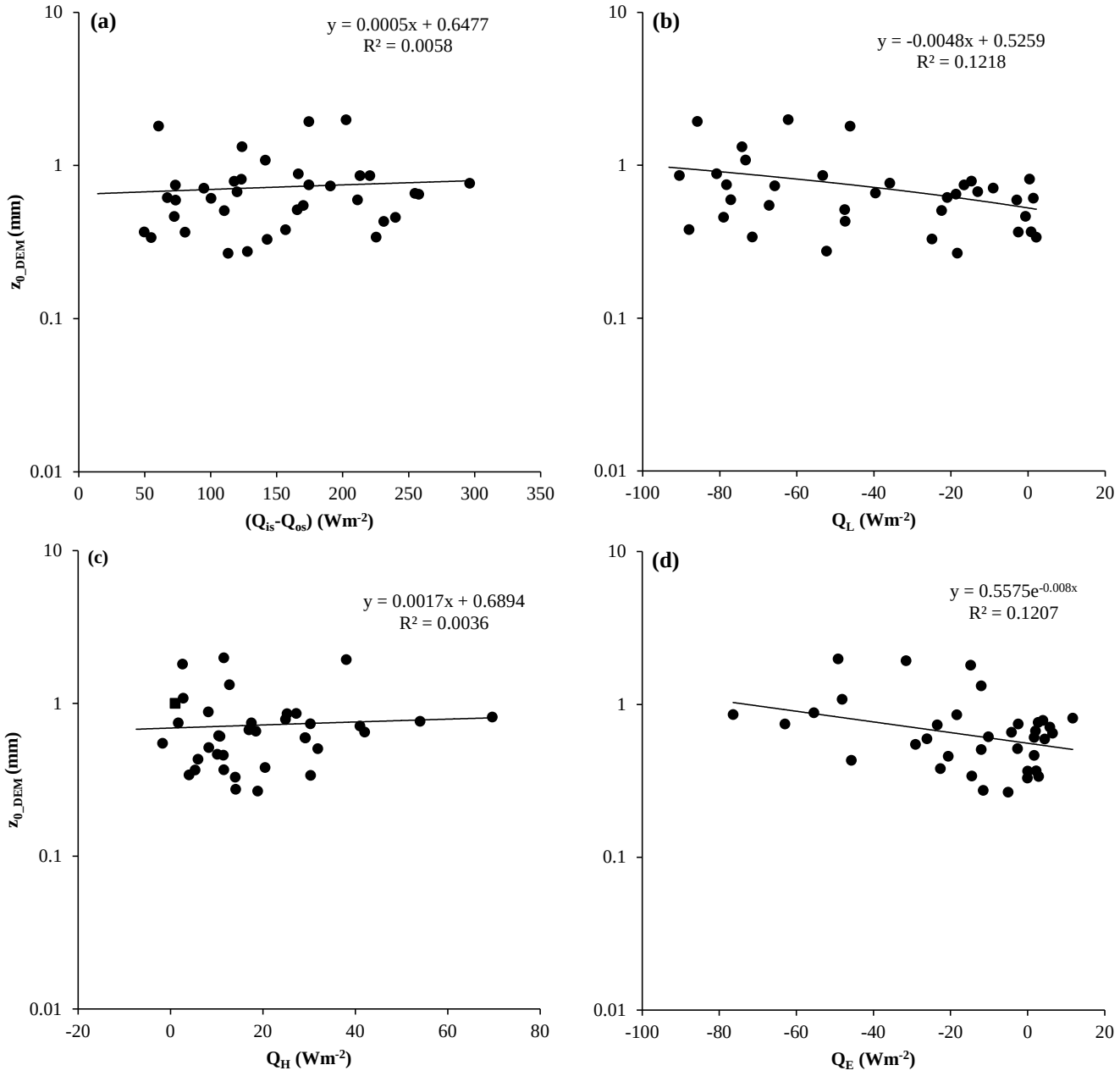

~~**Figure 10. Surface roughness vs. energy inputs. (a) Surface roughness vs. net shortwave radiation, (b) Surface roughness vs. net longwave radiation, (c) Surface roughness vs. sensible heat, (d) Surface roughness vs. latent heat.**~~

Figure 11. Daily upward wind direction DEM-based $z_{0\ DEM}$ vs. energy inputs. (a) $z_{0\ DEM}$ vs. net shortwave radiation, (b) $z_{0\ DEM}$ vs. net longwave radiation, (c) $z_{0\ DEM}$ vs. the bulk method calculated sensible heat, (d) $z_{0\ DEM}$ vs. the bulk method calculated latent heat.

Because net shortwave radiation and turbulent heat fluxes were the main energy fluxes affecting ice surface roughness, we calculated a turbulent heat proportion index:

$$L_S=(Q_H+Q_E+Q_P)/(Q_{is}-Q_{os}) \quad (5)$$

Note that aerodynamic surface roughness on days when snow fell was strongly affected by the amount of the snowfall. If we exclude snowfall days and snow covered period, we see a significant exponential relationship between ice surface z_{0_DEM} and L_S (Figure 12a, r= -0.34). Scatter diagrams showed significant exponential relationship between ice surface $z_{0\_Profile}$ and L_S and net longwave radiation (Figure12b, r=-0.69). $\bar{z}_{0\_DEM}$ vs. L_S also showed a significant exponential relationship (Figure 12c, r=-0.46). Scatter diagrams in Figure 12 also showed z_0 did not keep decreasing when L_S was above 0.2. z_{0_DEM}, $z_{0\_Profile}$ and $\bar{z}_{0\_DEM}$ was around 0.56±0.21mm, 0.33±0.03 mm and 0.6±0.26 mm, respectively.

The z_0 (z_{0_DEM}, $z_{0\_Profile}$ $\bar{z}_{0\_DEM}$) vs. L_S graph indicates that when turbulence and rainfall heat increased, aerodynamic surface roughness decreased. As soon as L_S is above 0.2, the ice surface will not keep smoothing and z_0 sustained its lowest stage. Time series correlation of all main energy items and $z_{0\_Profile}$ were performed. Table 4 shows an example of the lagged correlations between $z_{0\_profile}$ and five variables. The z_0 and net shortwave radiation displayed a positive correlation with 0 to 1 days lag time. The z_0 response to Q_E with a correlation of -0.6 showed a lag of 0 to 1 days. The $z_{0\_Profile}$ also had a negative relationship with Q_L with no lag or 1 day lag time. The $z_{0\_Profile}$ response to L_S with a correlation of -0.58 was with a lag of 0 to 2 days. 0 to 2 days lag time gives an indication of the main energy items efforts limitations over ice surface z_0. In other words, a sunny and cold day facilitates rough ice surfaces; warm and cloudy days tend to produce a smoother ice surface. When net shortwave radiation is higher, and if latent and sensible heat were smaller, z_0 would tend to be higher for the next 2 days. When net shortwave radiation is smaller, as on cloudy days, any snowfall or rainfall is usually associated with smaller z_0 for the following 2 days. Under a negative Q_M, the surface z_0 would be not affected by melting process.

~~We then graphed z_0 vs. L_S (see Figure 11). A strong exponential relationship was evident (Figure 11a, r= -0.45, P=0.002<0.005). Note that z_0 on days when snow fell was strongly affected by the amount of the snowfall. If we exclude snowfall days, we see an even more significant exponential relationship between z_0 and L_S (Figure 11b, r= -0.62, P=0.0001<0.001)).~~

~~The z_0 vs. L_S graph indicates that when turbulent and rainfall heat increased, roughness decreased. In other words, a sunny and cold day facilitates rough ice surfaces; warm and cloudy days tend to produce a smoother ice surface. When net shortwave radiation is higher, and if latent and sensible heat were higher, z_0 tends to be smaller; if latent and sensible heat were smaller, z_0 would tend to be higher. When net shortwave radiation is smaller, as on cloudy days, any snowfall or rainfall is usually associated with smaller z_0. Under a negative Q_M, the surface z_0 would be not affected by melting process.~~

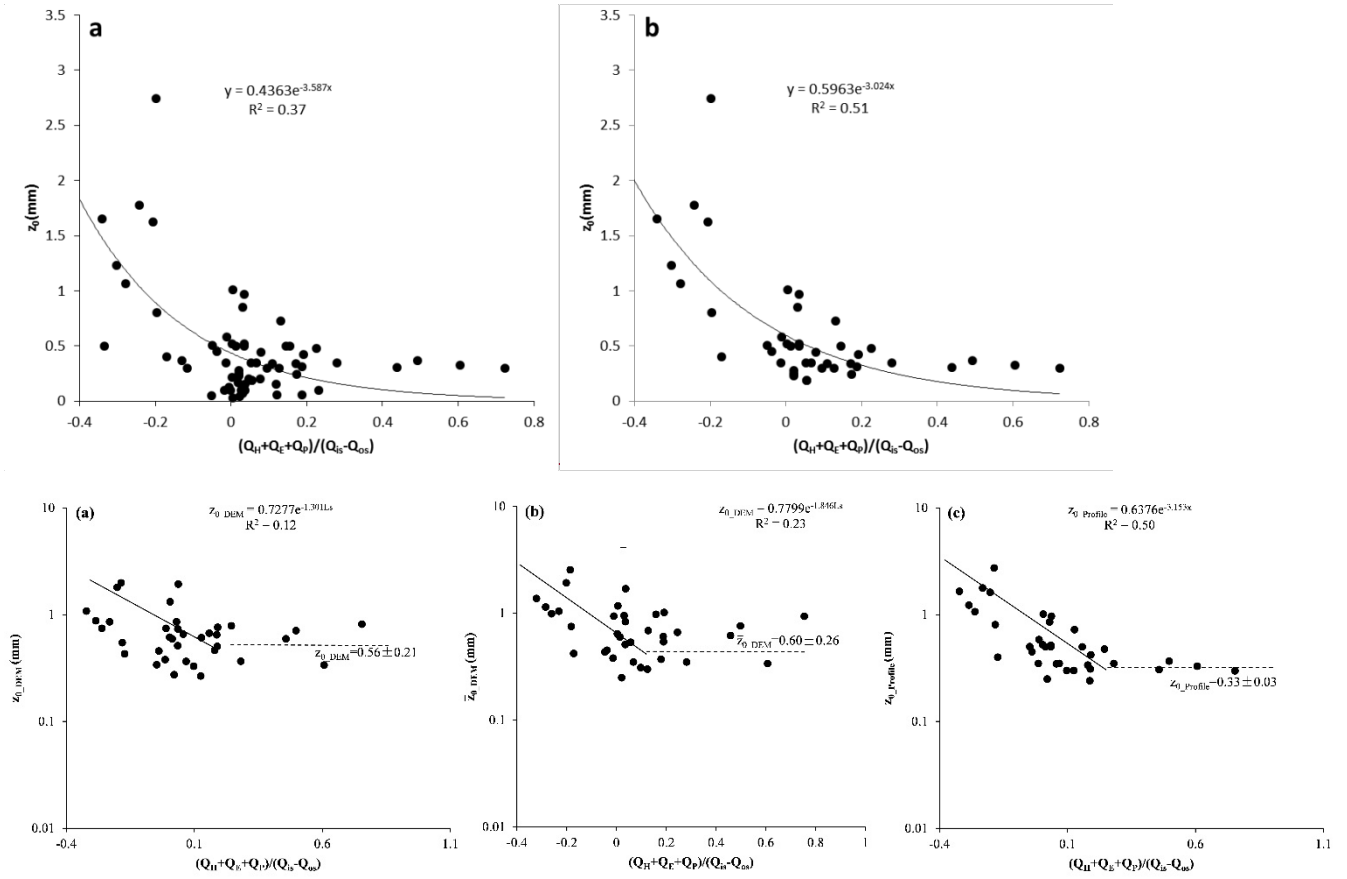

Figure 12. Aerodynamic surface roughness vs. L_s. Where $L_S=(Q_H+Q_E+Q_P)/(Q_{is}-Q_{os})$, in Figure 12(a) z_{0_DEM} was estimated based on prevailing upwind direction DEM based, in Figure 12(b) $\bar{z}_{0\_DEM}$ was the average of four cardinal wind directions z_0 to represent overall aerodynamic surface roughness, in Figure 12(c) $z_{0\_Profile}$ was the average of two orthogonal directions z_0. ~~Figure 11. Surface roughness vs. L_s. Where $L_S=(Q_H+Q_E+Q_P)/(Q_{is}-Q_{os})$, (a) Including snowfall days, (b) Excluding snowfall days.~~

Table 4 The lagged correlation between z_0 and the main energy items during the melting season, the sensible heat and latent heat here was calculated based on the bulk method.

$z_{0\_Profile}$	n	$(Q_{is}-Q_{os})$	Q_L	Q_E	Q_H	L_S
Lag-0	64	0.143	-0.309*	-0.614*	-0.088	-0.578*
Lag-1	63	0.131	-0.346*	-0.646*	-0.137	-0.572*
Lag-2	62	-0.022	-0.113	-0.356*	-0.307*	-0.585*
Lag-3	61	-0.144	0.051	-0.193*	-0.283*	-0.523*
Lag-4	60	-0.142	-0.241	-0.016	-0.013	-0.205

n= the number of samples, *P<0.05

4. Discussion

4.1 Automatic and manual photogrammetric methods

Photogrammetric techniques such as Structure from Motion (SfM) (James and Robson, 2012) and Multi-view Stereo (MVS) represent a low-cost option for acquiring high-resolution topographic data. Such approaches require relatively little training and are extremely inexpensive (Westoby et al., 2012; Fonstad et al., 2013;Passalacqua et al., 2015). We used both automatic and manual photogrammetric methods to sample spatial and temporal z_0 variation at the August-one ice cap. ~~One interesting finding:~~Adjustments to exposure time based on ice surface conditions and survey design of the area surrounding the target made the manual photogrammetry is more precise than automatic photogrammetry (Tables ~~1~~ 2 and ~~2~~3). However, precision is not always the major concern. The glacier surface was a harsh, even punishing environment for the researchers doing manual photogrammetry. In addition, manual photogrammetry took much longer. Automatic methods reduced hours of field work, spared researchers, and produced nearly continuous data. Cloudy or frosty weather affected automatic photogrammetry exposures, and heavy snowfalls resulted in a texture-less surface. Nevertheless, it is likely that photogrammetry techniques will continue to improve and that these drawbacks may be mitigated.

4.2 Spatial and temporal variability of z_0

Previous studies of glacier surfaces roughness ~~rarely~~ have rarely covered the whole glacier, from terminals to top, in one melting season (Föhn, 1973; Smeets et al., 1999; Denby and Smeets, 2000; Greuell and Smeets, 2001; Albert and Hawley, 2002; Brock et al., 2006; Smeets and Van den Broeke, 2008; Smith et al., 2016). This ~~W~~whole-glacier study allowed us to follow the movement of the transition zone, where snow was melting and exposing ice, from terminals to top. The transition zone moved up as the melting season proceeded, so roughening the surface of the glacier and raising z_0. At the start of the melting season, snow cover first disappeared, leaving an ice surface, at the ~~terminal~~terminals end of the August-one ice cap, ~~glacier,~~ that is, at the lower altitude. This newly exposed surface was rougher (z_0 was higher) than on the upper part of glacier, which was still snow covered (see the black line Figure 6a for z_0 distribution at different altitudes). As the snowline shifted to higher altitudes, ice surface increased, as did z_0 (see the dashed black curve in Figure 6b). As the melting continued, the snow and ice transition belt reached the top of glacier (see the dotted curve in Figure 6c). When the ~~glacier~~ ice cap was completely free of snow, z_0 and elevation were no longer correlated (see the dotted-dashed line in Figure 6d). In summary, maximum z_0 was recorded at the cross-glacier transition zone between snow and ice. This zone shifted from lower altitude to higher altitude, from terminals to top, during the melting season. The spatial pattern of z_0 distribution affected turbulent fluxes. The transition zone had maximum z_0 and the zone also migrated across much of the glacier, highlighting the importance of transient surface characteristics.

Micro-topography, wind profile, and eddy covariance methods generate a wide range of z_0 values for snow and ice surfaces (Grainger and Lister, 1966; Munro, 1989; Bintanja and Broeke et al., 1995; Schneider, 1999; Hock and Holmgren, 2005; Brock et al., 2006; Andreas et al., 2010; Gromke et al., 2011).~~(Föhn, 1973;Smeets et al., 1999;Irvine-Fynn et al., 2014)~~, ~~wind profile,~~

~~and eddy covariance methods generate a wide range of z_0 values for snow and ice surfaces (Brock et al., 2006).~~ In this study, $z_{0\_profile}$, z_{0_DEM}, and $\bar{z}_{0\_DEM}$ showed similar variation pattern during the melting season. The difference of $z_{0\_profile}$, z_{0_DEM}, and $\bar{z}_{0\_DEM}$ were within one order of magnitude. The latent and sensible heat calculated by $z_{0\_profile}$, z_{0_DEM}, and $\bar{z}_{0\_DEM}$ were highly relevant among these methods. The automatic photogrammetry estimated z_0 for snow-covered surfaces ranged from 0.1 to 0.55. New snowfall at snow surface in July formed the lowest z_0 values. Previous studies have shown that freshly fallen snow is subject to rapid destructive metamorphism (McClung and Schaerer, 2006), which can dramatically change the roughness of fresh snow surfaces (Fassnacht et al., 2009b). Our study showed that z_0 followed an increasing trend during melting season. Intermittent snowfall first decreased snow surface z_0, which then began to increase as the snow surface deteriorated. In the data from Clifton et al. (2008), snow surface z_0 was estimated at between 0.17 to 0.6 mm in a wind tunnel experiment. In an analysis of ultra-sonic anemometer recorder data over snow-covered sea-ice, Andreas et al. (2010) found z_0 values ranging from 10^{-2} to 10^{1} mm. In a wind-tunnel experiment of fresh snow with no-drift conditions, Gromke et al. (2011) estimated z_0 to be lying between 0.17 to 0.33 mm with no apparent dependency on the friction velocity. Our snow surface data showed z_0 values fluctuated between 0.03 to 0.55 mm, consistent with some of those wind-tunnel studies. The scatter of z_0 data reported in some studies is quite large, with a range of 10^{-2} to 10^{1} mm. The result may be attributed to the occurrence of snow drift, a transitional rough-flow regime and large uncertainties in the estimation of friction velocities that propagate to the computation of z_0 (Andreas et al., 2010; Gromke et al., 2011). On the contrary, the small scatter in our data was induced only by the natural variability of snow-surface roughness.

For patchy snow-covered ice surfaces, z_0 varied from 0.5 to 2.6mm and ice surface z_0 varied from 0.24 to 1.1mm. During the melting season, there were no blowing snow events and snow surface z_0 was relatively smaller than in patchy snow-covered surface or ice surface. Ice surface z_0 was generally larger than snow surface and smaller than patch snow-covered surface. Our results match values reported in studies reporting results ranging from. 0.1mm to 6.9mm in Qilian mountain glaciers (Guo et al., 2018;Sun et al., 2018). Our results showed that z_0 reached its maximum at the end of the summer melt, which matched wind profile measurements by Smeets and Broeke (2008).~~It should be noted that *averaged* values for z_0 matched those found in other studies. Z_0 for *snow-covered* surfaces ranged from 0.01 to 3.5mm (mean: 0.5mm). These results match values reported in other studies, which ranged from 0.1 to 8.2 mm (Munro, 1989;Hock and Holmgren, 2005;Schneider, 1999;Grainger and Lister, 1966).~~

~~Z_0 for *ice surfaces* ranged from 0.01 to 2.5mm (mean: 0.6). Our results also match values reported in studies reporting results ranging from. 0.1mm to 6.9mm (Brock et al., 2006;Guo et al., 2018;Sun et al., 2018). Our results showed that z_0 reached its maximum at the end of the summer melt, which matched indirect measurements by Smeets and Broeke (2008).~~

~~Previous studies have shown that freshly fallen snow is subject to rapid destructive metamorphism (McClung and Schaerer, 2006), which can dramatically change the roughness of fresh snow surfaces (Fassnacht et al., 2009b). Our study showed that z_0 could be quite variable during melting season. Intermittent snowfall first decreased snow surface z_0, which then began to increase as the snow surface deteriorated. With the appearance of cryoconite, z_0 rose to its greatest value.~~

The aerodynamic surface roughness is influenced by both boundary layer and the surface. In this study, the microtopographic estimated aerodynamic surface roughness only considers surface topography at plot scale, but its variability influenced by its surroundings. Thus, the results of z_0 estimated in this study still need validated by wind tower or eddy covariance observations.

However, microtopographic roughness metrics are a very strong proxy for z_0 (e.g. Nield et al, 2013), so we have much more confidence in the temporal and spatial variability presented by this work.

4.3 Effects of surface energy balance components on aerodynamic surface roughness

Aerodynamic roughness is associated with the geometry of ice roughness elements (Kuipers, 1957;Lettau, 1969;Munro, 1989). Surface geometry roughness develops due to local melt inhomogeneities in melting season. In early work, researchers argued that a variety of ablation forms, such as sun cups, penitents, cryoconite holes or dirt cones are formed by the sun (Matthes, 1934; Lliboutry, 1954; Mcintyre, 1984; Rhodes et al., 1987; Betterton, 2000). These ablation forms develop in regions with bright sunlight and cold, dry weather conditions are apparently required (Rhodes et al., 1987). These structures are observed to decay if the weather is cloudy or very windy (Matthes, 1934; Lliboutry, 1954; Mcintyre, 1984). ~~In this study, our results show that L_s (turbulent heat index; see Section 3.5.5, equation 5) is a determining factor in directly measured z_0. A high index was associated with a smooth ice surface; a low or even a negative index was associated with rough surfaces. Hence at the end of melting season, ice surfaces would be at their very roughest when L_s reached to its lowest.~~

The August-one ice cap dust concentrations are high in the melting season.~~is a heavy loading glacier; c~~Cryoconites are unevenly distributed over the ice surface leading to differential absorption of shortwave radiation at microscale. This process results in the roughening of the ice surface; a process that enhances turbulent heat exchange across the atmospheric boundary layer-ice interface. When the air temperature is above 0 °C, the ice surface keeps melting. The turbulent heat smooths the ice surface and increases the cryoconite concentration over the ice surface and decreases ice surface albedo, enhancing shortwave radiation absorption (Figure 9). This roughening and smoothing process makes ice surface z_0 to fluctuate at around 0.56 mm as long as the air temperature is above 0 °C. When temperature drops below 0 °C, bright sunlight and dry weather shutdown the ice surface smoothing process. The shortwave radiation induces even rougher ice and larger z_0 until snow covers the ice surface. At the August-one ice cap, the turbulent heat contributes a small portion of incoming energy, but the smoothing ice surface process decreases ice surface albedo and seems enhance ice surface shortwave radiation. The z_0 fluctuation in the melt season is similar with cryoconite holes developing when the radiative flux is dominant and decaying when turbulent heat is dominant (McIntyre, 1984; Takeuchi et al., 2018). The glacier surface energy balance components vs. z_0 analysis in this study confirms that main energy items of net shortwave radiation and turbulent heat flux affect the same day and following 2 days z_0. This study found an exponential relationship between z_0 and L_S. The delicate role of z_0 played in the ice surface balance is still not fully known. Further comparative studies are needed to investigate the z_0 variation through eddy covariance, profile method and DEM-based z_0 estimation.~~ On clear days shortwave radiation caused heterogeneous melt: cryoconite-covered ice quickly melted and formed rough ice surfaces. Under cloudy or rainy days, turbulent heat is dominant, and ice surface roughness decreased. This process resembles the process by which cryoconite holes develop and decay. In that process, cryoconite holes develop when the radiative flux is dominant and decay when turbulent heat is dominant (McIntyre, 1984;Takeuchi et al., 2018).~~

~~This study found an exponential relationship between z_0 and L_s. These results suggest that quantitative rather than qualitative research will be of great help to researchers hoping to understand ice surface roughness.~~

5. Conclusions

Manual and automatic measurements of snow and ice surface roughness at the August-one ice cap showed ~~great~~ spatial and temporal variation in z_0 over the melting season. Manual measurements, taken from terminals to glacier top, show that the nature of the surface cover features are correlated with z_0 rank in this order: transition region > pure ice area or pure snow area. The transition region forms a zone of maximum z_0, which shifts, over the melting season, from terminals to top. The observed z_0 vs energy items analysis indicated that L_S (turbulent heat index) was also an important determinant of ice aerodynamic surface roughness.

Aerodynamic ~~S~~surface roughness is a major parameter in calculations of glacier-surface turbulent heat fluxes. In previous studies investigators used a constant z_0 value for the whole surface of the glacier. This study captures much smaller scale variation spatial and temporal glacier surface aerodynamic roughness through automatic and manual photogrammetric observations. Such close observation of variation in z_0 certainly enhanced the accuracy of the surface energy balance models developed in the course of this study.

Of course, this study carried out at the ice cap with neat ordering of the annual layers. The August-once ice cap moved slowly and no crevasses were formed over the ice cap and channels were not considered in this study. In this case, a moderate variation of z_0 was estimated than it would be for debris covered glaciers (Miles et al., 2017; Quincey et al., 2017). Uneven or heterogeneous ice surface such as sastrugis, crevasses, channels, and penitents could greatly affect ice surface aerodynamic surface roughness and it would be hard to estimate its z_0 based on a profile method. SfM estimation of z_0 might be a good choice at macro-scale. In the accumulation season, more attention would be needed to be paid to spatial and temporal variations of z_0 as z_0 is a key parameter for sublimation calculation during this period. Studies have indicated that the Lettau (1969) approach calculated z_0 dependent on plot scale and resolution. In this study, we only select 1×1 m scale at 1mm resolution to study its spatial and temporal variability. Further comparative studies of z_0 are needed at different scales and resolutions. ~~covered only one glacier. It is not clear that it is typical of other Qilian glaciers, or of glaciers in the rest of the world. Further studies are necessary.~~

Acknowledgements

This study was supported by the National Natural Sciences Foundation of China (41877163, 41671029). We thank the two reviewers for their insightful comments and ideas to improve the paper.

References

Albert, M. R., and Hawley, R. L.: Seasonal changes in snow surface roughness characteristics at Summit, Greenland: implications for snow and firn ventilation, Annals of Glaciology, 35, 510-514, 10.3189/172756402781816591, 2002.

Andreas, E. L.: Parameterizing scalar transfer over snow and ice: A review, Journal of Hydrometeorology, 3, 417-432, 2002.

Andreas, E. L., Persson, P. O. G., Jordan, R. E., Horst, T. W., Guest, P. S., Grachev, A. A., and Fairall, C. W.: Parameterizing turbulent exchange over sea ice in winter, Journal of Hydrometeorology, 11:87–104, doi.org/10.1175/2009JHM1102.1, 2010.

Arck, M., and Scherer, D.: Problems in the determination of sensible heat flux over snow, Geografiska Annaler, 84, 157‐169, 10.1111/1468-0459.00170, 2002.

Betterton, M. D.: Formation of structure in snowfields: Penitentes, suncups, and dirt cones, 1-28, arXiv:physics/0007099v1 [physics.geo-ph] 31 Jul 2000, 2000.

Bintanja, R., and Van den Broeke, M.: Momentum and scalar transfer-coefficients over aerodynamically smooth Antarctic surfaces. Boundary-Layer Meteorology, 74, 89–111. doi.org/10.1007/BF00715712, 1995.

Brock, B. W., Willis, I. C., and Sharp, M. J.: Measurement and parameterization of aerodynamic roughness length variations at Haut Glacier d'Arolla, Switzerland, Journal of Glaciology, 52, 1-17, 2006.

Bruce, D., and Smeets, C. J. P. P.: Derivation of turbulent flux profiles and roughness lengths from katabatic flow dynamics, Journal of applied Meteorology, 39, 12, 2000.

Chen, R.S., Song, Y. X., Kang, E. S., Han, C. T., Liu, J. F., Yang, Y., Qing, W. W., and Liu, Z. W.: A Cryosphere-Hydrology Observation System in a Small Alpine Watershed in the Qilian Mountains of China and Its Meteorological Gradient, Arctic, Antarctic, and Alpine Research, 46, 505–523, 10.1657/1938-4262-46.2.505, 2014.

Clifton, A., Manes. C., Rueedi, J.D., Guala, M., and Lehning, M.: On shear-driven ventilation of snow. Boundary-Layer Meteorol 126:249–261, doi.org/10.1007/s10546-007-9235-0, 2008.

Denby, B., and Smeets, C.: Derivation of turbulent flux profiles and roughness lengths from katabatic flow dynamics, Journal of applied Meteorology, 39, 1601-1612, 2000.

Denby, B., and Snellen, H.: A comparison of surface renewal theory with the observed roughness length for temperature on a melting glacier surface, Boundary-layer meteorology, 103, 459-468, 2002.

Dong, W. P., Sullivan, P. J., and Stout, K. J.: Comprehensive study of parameters for characterizing three-dimensional surface topography I: Some inherent properties of parameter variation, Wear, 159, 161-171, 1992.

Föhn, P. M. B.: Short-term snow melt and ablation derived from heat-and mass-balance measurements, Journal of Glaciology, 12, 275-289, 1973.

Fassnacht, S. R., Stednick, J. D., Deems, J. S., and Corrao, M. V.: Metrics for assessing snow surface roughness from digital imagery, Water Resources Research, 45, W00D31, 10.1029/2008wr006986, 2009a.

Fassnacht, S. R., Williams, M., and Corrao, M.: Changes in the surface roughness of snow from millimetre to metre scales, Ecological Complexity, 6, 221-229, 10.1016/j.ecocom.2009.05.003, 2009b.

Fitzpatrick, N., Radić, V., and Menounous, B.: A multi-season investigation of glacier surface roughness lengths through in situ and remote observation, The Cryosphere, 13, 1051-1071, 10.5194/te-13-1051-2019, 2019.

Föhn, P. M. B.: Short-term snow melt and ablation derived from heat-and mass-balance measurements, Journal of Glaciology, 12, 275-289, 1973.

Fonstad, M. A., Dietrich, J. T., Courville, B. C., Jensen, J. L., and Carbonneau, P. E.: Topographic structure from motion: a new development in photogrammetric measurement, Earth Surface Processes and Landforms, 38, 421-430, 10.1002/esp.3366, 2013.

Garratt, J. R.: The Atmospheric Boundary Layer. New York: Cambridge University Press, 1992.

Grainger, M., and Lister, H.: Wind speed, stability and eddy viscosity over melting ice surfaces, Journal of Glaciology, 6, 1966.

Greuell, W., and Smeets, P.: Variations with elevation in the surface energy balance on the Pasterze (Austria), Journal of Geophysical Research: Atmospheres, 106, 31717-31727, 2001.

Gromke, C., Manes, C., Walter B, Lehning, M., and Guala, M.: Aerodynamic roughness length of Fresh snow, Boundary-Layer Meteorology, 141, 21-34, 10.1007/s10546-011-9623-3, 2011.

Guo, S. h., Chen, R. s., Liu, G. h., Han, C. t., Song, Y. x., Liu, J. f., Yang, Y., Liu, Z. w., Wang, X. q., and Liu, X. ~~j~~J.: Simple Parameterization of Aerodynamic Roughness Lengths and the Turbulent Heat Fluxes at the Top of Midlatitude August‐One Glacier, Qilian Mountains, China, Journal of Geophysical Research: Atmospheres, 123, 12,066-012,080, 10.1029/2018JD028875, 2018.

Guo, W., Liu, S., Xu, J., Wu, L., Shangguan, D., Yao, X., Wei, J., Bao, W., Yu, P., Liu, Q., and Jiang, Z.: The second Chinese glacier inventory: data, methods and results. Journal of Glaciology, Journal of Glaciology, 61, 10.3189/2015jog14j209, 2015.

Hock, R., and Holmgren, B.: A distributed surface energy-balance model for complex topography and its application to Storglaciären, Sweden, Journal of Glaciology, 51, 25-36, 10.3189/172756505781829566, 2005.

Irvine-Fynn, T., Sanz-Ablanedo, E., Rutter, N., Smith, M., and Chandler, J.: Measuring glacier surface roughness using plot-scale, close-range digital photogrammetry, Journal of Glaciology, 60, 957-969, 10.3189/2014JoG14J032, 2014.

James, M. R., and Robson, S.: Mitigating systematic error in topographic models derived from UAV and ground-based image networks, Earth Surface Processes and Landforms, 39, 1413-1420, DOI: 10.1002/esp.3609, 2014.

James, M. R., Robson, S., and Smith, M., W.: 3-D uncertainty-based topographic change detection with structure-from-motion photogrammetry: precision maps for ground control and directly georeferenced surveys, Earth Surface Processes and Landforms, 42, 1769-1788, 10.1002/esp.4125, 2017.

James, M., and Robson, S.: Straightforward reconstruction of 3D surfaces and topography with a camera: Accuracy and geoscience application, Journal of Geophysical Research: Earth Surface, 117, F03017, 10.1029/2011JF002289, 2012.

Javernick, L., Brasington, J., and Caruso, B.: Modeling the topography of shallow braided rivers using Structure-from-Motion photogrammetry, Geomorphology, 213, 166-182, 10.1016/j.geomorph.2014.10.006, 2014.

~~Kääb, A., and Vollmer, M.: Surface geometry, thickness changes and flow fields on permafrost streams: automatic extraction by digital image analysis, Permafrost and Periglacial Processes, 11, 10.1002/1099-1530(200012)11:4<315::AID-PPP365>3.0.CO;2-J, 2000.~~

Konya, K., and Matsumoto, T.: Influence of weather conditions and spatial variability on glacier surface melt in Chilean Patagonia, Theoretical and applied climatology, 102, 139-149, 2010.

Kuipers, H.: A relief meter for soil cultivation studies, Netherlands Journal of Agricultural Science, 5, 255-262, 1957.

Lacroix, P., Legrésy, B., Coleman, R., Dechambre, M., and Rémy, F.: Dual-frequency altimeter signal from Envisat on the Amery ice-shelf, Remote Sensing of Environment, 109, 285-294, 10.1016/j.rse.2007.01.007, 2007.

Lacroix, P., Legrésy, B., Langley, K., Hamran, S., Kohler, J., Roques, S., Rémy, F., and Dechambre, M.: In situ measurements of snow surface roughness using a laser profiler, Journal of Glaciology, 54, 753-762, 10.3189/002214308786570863, 2008.

Lehning, M., Bartelt, P., Brown, B., and Fierz, C.: A physical SNOWPACK model for the Swiss avalanche warning: Part III: meteorological forcing, thin layer formation and evaluation, Cold Regions Science and Technology, 35, 10.1016/S0165-232X(02)00072-1, 2002.

Lettau, H.: Note on aerodynamic roughness parameter estimation the basis of roughness element description, Journal of Applied Meteorology, 8, 1969.

Manninen, T., Anttila, K., Karjalainen, T., and Lahtinen, P.: Automatic snow surface roughness estimation using digital photos, Journal of Glaciology, 58, 993-1007, 10.3189/2012JoG11J144, 2012.

McClung, D., and Schaerer, P. A.: The avalanche handbook, The Mountaineers Books, Seattle, WA, 2006.

McIntyre, N. F.: Cryoconite hole thermodynamics, Canadian Journal of Earth Sciences, 21, 1984.

Miles, E. S., Steiner, J. F., and Brun, F.: Highly variable aerodynamic roughness length (z_0) for a hummocky debris-covered glacier, Journal of Geophysical Research: Atmospheres, 122, 8447-8466, 10.1002/2017JD026510, 2017.

Munro, D. S.: Surface roughness and bulk heat transfer on a glacier: comparison with eddy correlation, Journal of Glaciology, 35, 343-348, 10.3189/S0022143000009266, 1989.

Nield, J. M., King, J., Wiggs G. F. S., Leyland, J., Bryant, R. G., Chiverrell, R. C., Darby, S. E., Eckardt, F. D., Thomas, D. S. G., Vircavs, L. H., and Washington, R.: Estimating aerodynamic roughness over complex surface terrain, Journal of Geophysical Research: Atmospheres, 118, 12948-12961, 10.1002/2013JD020632, 2013.

Oke, T. R.: Boundary layer climates, Routledge, London, 1987.

Oveisgharan, S., and Zebker, H. A.: Estimating snow accumulation from InSAR correlation observations, IEEE Transactions on Geoscience and Remote Sensing, 45, 10-20, 10.1109/TGRS.2006.886196, 2007.

Passalacqua, P., Belmont, P., Staley, D. M., Simley, J. D., Arrowsmith, J. R., Bode, C. A., Crosby, C., DeLong, S. B., Glenn, N. F., Kelly, S. A., Lague, D., Sangireddy, H., Schaffrath, K., Tarboton, D., Wasklewicz, T., and Wheaton, J. M.: Analyzing high resolution topography for advancing the understanding of mass and energy transfer through landscapes: A review, Earth-Science Reviews, 148, 174-193, 10.1016/j.earscirev.2015.05.012, 2015.

Quincey, D., Smith, M., Rounce, D., Ross, A., King, O., and Watson, C.: Evaluating morphological estimates of the aerodynamic roughness of debris covered glacier ice, Earth surface processes and landforms, 42, 2541-2553, 10.1002/esp.4198, 2017.

Rees, W. G., and Arnold, N. S.: Scale-dependent roughness of a glacier surface: implications for radar backscatter and aerodynamic roughness modelling, Journal of Glaciology, 52, 214-222, 10.3189/172756506781828665, 2006.

Rippin, D. M., Pomfret, A., and King, N.: High resolution mapping of supra - glacial drainage pathways reveals link between micro - channel drainage density, surface roughness and surface reflectance, Earth Surface Processes and Landforms, 40, 1279-1290, 10.1002/esp.3719, 2015.

Rhodes, J. J., Armstrong, R. L., and Warren, S. G.: Mode of formation of “ablation hollows” controlled by dirt content of snow, Journal of Glaciology, 33, 135-139, 1987.

Rippin, D. M., Pomfret, A., and King, N.: High resolution mapping of supra - glacial drainage pathways reveals link between micro - channel drainage density, surface roughness and surface reflectance, Earth Surface Processes and Landforms, 40, 1279-1290, 10.1002/esp.3719, 2015.

Rounce, D. R., Quincey, D. J., and McKinney, D. C.: Debris-covered glacier energy balance model for Imja–Lhotse Shar Glacier in the Everest region of Nepal, The Cryosphere, 9, 2295–2310, 10.5194/tc-9-2295-2015, 2015.

Schneider, C.: Energy balance estimates during the summer season of glaciers of the Antarctic Peninsula Global Planetary Change, 22, 10.1016/S0921-8181(99)00030-2, 1999.

Smeets, C. J. P. P., and Van den Broeke, M. R.: Temporal and spatial variations of the aerodynamic roughness length in the ablation zone of the Greenland ice sheet, Boundary-layer meteorology, 128, 315-338, 10.1007/s10546-008-9291-0, 2008.

Smeets, C. J. P. P., Duynkerke, P. G., and Vugts, H. F.: Turbulence characteristics of the stable boundary layer over a mid-latitude glacier. Part II: Pure katabatic forcing conditions, Boundary-layer meteorology, 97, 73-107, 2000.

Smeets, C., Duynkerke, P., and Vugts, H.: Observed wind profiles and turbulence fluxes over an ice surface with changing surface roughness, Boundary-Layer Meteorology, 92, 101-121, 1999.

Smith, M. W., Quincey, D. J., Dixon, T., Bingham, R. G., Carrivick, J. L., Irvine - Fynn, T. D. L., and Rippin, D. M.: Aerodynamic roughness of glacial ice surfaces derived from high - resolution topographic data, Journal of Geophysical Research: Earth Surface, 121, 748-766, 10.1002/2015JF003759, 2016.

Smith, M. W.: Roughness in the earth sciences, Earth-Science Reviews, 136, 202-225, 2014.

Steiner, J. F., Litt, M., Stigter E. E., Shea, J., Bierkens M. F. P., and Immerzeel W. W.: The importance of turbulent fluxes in the surface energy balance of a debris-covered glacier in the Himalayas, Frontiers in Earth Science, 6, 144, 10.3389/feart.2018.00144 2018.

Sun, W. j., Qin, X., Wang, Y. t., Chen, J. z., Du, W. t., Zhang, T., and Huai, B. j.: The response of surface mass and energy balance of a continental glacier to climate variability, western Qilian Mountains, China, Climate dynamics, 50, 3557-3570, 10.1007/s00382-017-3823-6, 2018.

Takeuchi, N., Sakaki, R., Uetake, J., Nagatsuka, N., Shimada, R., Niwano, M., and Aoki, T.: Temporal variations of cryoconite holes and cryoconite coverage on the ablation ice surface of Qaanaaq Glacier in northwest Greenland, Annals of Glaciology, 59, doi: 10.1017/aog.2018.19, 2018.

Wendler, G., and Streten, N.: A short term heat balance study on a coast range glacier, pure and applied geophysics, 77, 68-77, 1969.

Westoby, M. J., Brasington, J., Glasser, N.F., Hambrey, M. J., and Reynolds, J. M.: 'Structure-from-Motion' photogrammetry: A low-cost, effective tool for geoscience applications. Geomorphology, 179, 300-314, 10.1016/j.geomophy.2012.08.021, 2012.